GEOHORIZONS

Crustal insights from gravity and aeromagnetic analysis: Central North Slope, Alaska

Richard W. Saltus, Christopher J. Potter, and Jeffrey D. Phillips

ABSTRACT

Aeromagnetic and gravity data are processed and interpreted to reveal deep and shallow information about the crustal structure of the central North Slope, Alaska. Regional aeromagnetic anomalies primarily reflect deep crustal features. Regional gravity anomalies are more complex and require detailed analysis. We constrain our geophysical models with seismic data and interpretations along two transects including the Trans-Alaska Crustal Transect. Combined geophysical analysis reveals a remarkable heterogeneity of the pre-Mississippian basement. In the central North Slope, pre-Mississippian basement consists of two distinct geophysical domains. To the southwest, the basement is dense and highly magnetic; this basement is likely mafic and mechanically strong, possibly acting as a buttress to basement involvement in Brooks Range thrusting. To the northeast, the central North Slope basement consists of lower density, moderately magnetic rocks with several discrete regions (intrusions?) of more magnetic rocks. A conjugate set of geophysical trends, northwest-southeast and southwest-northeast, may be a factor in the crustal response to tectonic compression in this domain. High-resolution gravity and aeromagnetic data, where available, reflect details of shallow fault and fold structure. The maps and profile models in this report should provide useful guidelines and complementary information for regional structural studies, particularly in combination with detailed seismic reflection interpretations. Future challenges include collection of high-resolution gravity and aeromagnetic data for the entire North Slope as well as additional deep crustal information from seismic, drilling, and other complementary methods.

Manuscript received April 14, 2005; provisional acceptance July 13, 2005; revised manuscript received May 2, 2006; final acceptance May 9, 2006.
DOI:10.1306/05090605066

AUTHORS

RICHARD W. SALTUS ~ *U.S. Geological Survey, Mail Stop 964, Box 25046, Denver, Colorado 80225; saltus@usgs.gov*

Rick Saltus has worked since 1980 as a geophysicist for the U.S. Geological Survey. His work primarily involves the application of gravity and magnetic methods to geologic, tectonic, and resource assessment studies. He graduated from Stanford University (M.S., 1988; Ph.D., 1991). He has contributed to the U.S. Geological Survey energy assessments of northern and central Alaska.

CHRISTOPHER J. POTTER ~ *U.S. Geological Survey, Mail Stop 939, Box 25046, Denver, Colorado 80225; cpotter@usgs.gov*

Chris Potter, a structural geologist, has been employed at the U.S. Geological Survey since 1989. Chris received graduate degrees from Brown University (M.S., 1976) and the University of Washington (Ph.D., 1983), before spending several years as a research associate at Cornell University and assistant professor at Lafayette College. Most of his research involved regional studies in the North American Cordillera and central United States, commonly integrating field geologic studies with seismic reflection and other geophysical data. He has been working on structural interpretations and hydrocarbon assessments on the North Slope of Alaska for the past 10 years.

JEFFREY D. PHILLIPS ~ *U.S. Geological Survey, Mail Stop 964, Box 25046, Denver, Colorado 80225; jeff@usgs.gov*

Jeff Phillips has worked as a research geophysicist with the U.S. Geological Survey since 1975, specializing in potential-field theory and its application to geologic problems, including water, mineral, and energy resources. He received his graduate degrees from Stanford University (M.S., 1973; Ph.D., 1975). He has participated in U.S. Geological Survey energy assessment studies of northern and central Alaska.

ACKNOWLEDGEMENTS

We thank U.S. Geological Survey reviewers Bob Jachens and Ken Bird for the extremely constructive comments and corrections to the initial manuscript. Bob Morin (U.S. Geological Survey) performed data reduction and quality control checking for regional gravity data. AAPG reviews by Eli Silver, Phil Armstrong, and Ernie Mancini significantly improved the focus and readability of the article.

INTRODUCTION

The central North Slope of Alaska encompasses the territory between the Colville and Canning rivers (Figure 1). The southern boundary is the Brooks Range mountain front. We discuss geophysical data and interpretations for the central North Slope as well as parts of the National Petroleum Reserve, Alaska (NPRA) to the west, parts of the Brooks Range to the south, and parts of the Arctic National Wildlife Refuge (ANWR) to the east. Topographically, the central North Slope includes the Brooks Range foothills and the broad Arctic coastal plain dotted with lakes. The crest of the western Brooks Range trends west to east and then bends near Atigun Gorge (where the Dalton Highway passes through; Figure 1) and follows a more northeasterly trend in the east.

The northern part of the central North Slope has been extensively probed with geophysical surveys (primarily seismic reflection) and exploratory drilling. About 260 wildcat wells had been drilled in the area north of 70°N between the Colville and Canning rivers and in the adjacent offshore through the end of 1999. Since 1999, about 20 additional exploratory wells have been drilled in this area. The current oil exploration and development region, associated with the Prudhoe and related fields, extends about 24 km (15 mi) inland along the Beaufort Sea coast from the Canning River to the Colville River. The remainder of the central North Slope has been only sparsely tested by drilling,

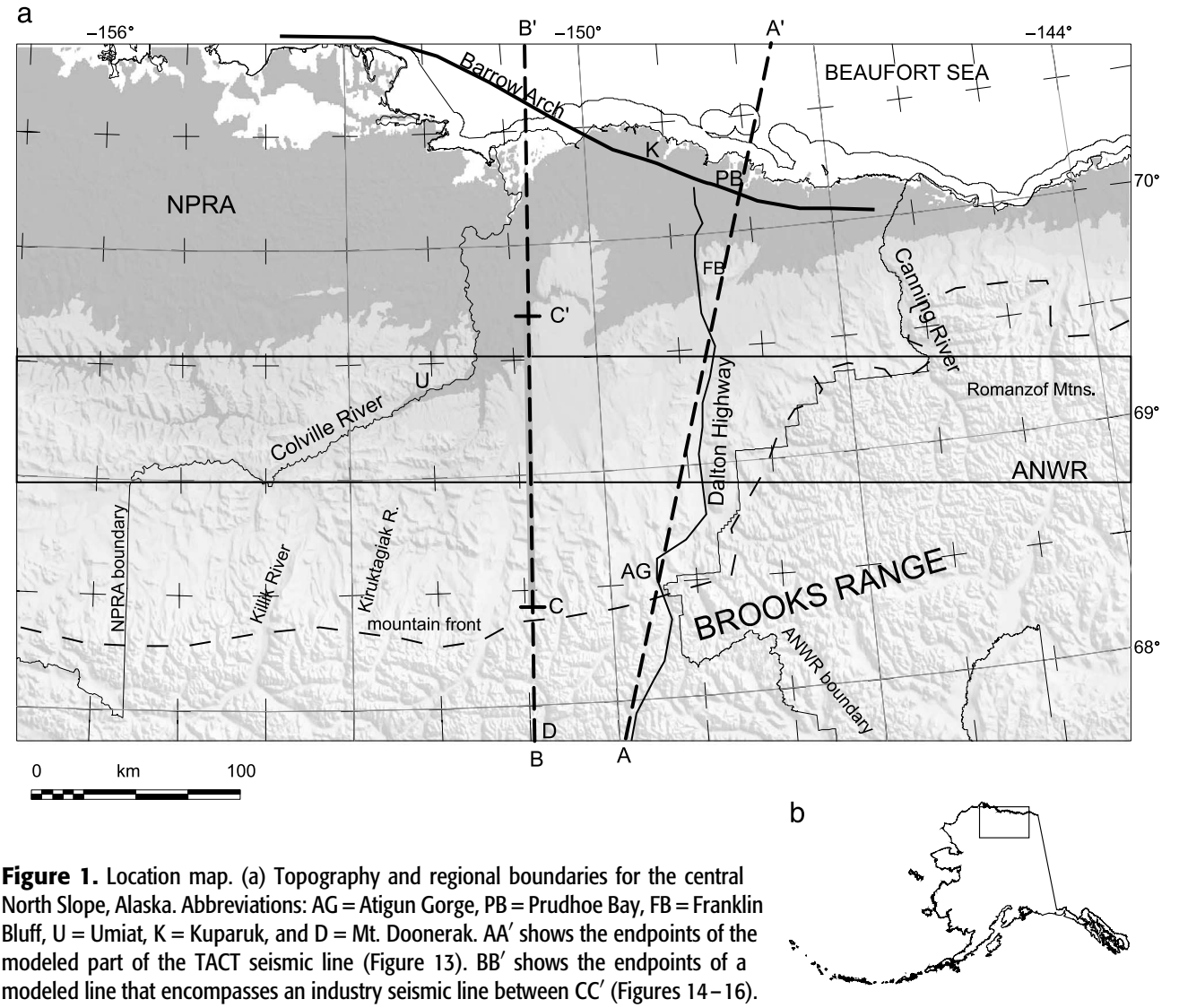

Figure 1. Location map. (a) Topography and regional boundaries for the central North Slope, Alaska. Abbreviations: AG = Atigun Gorge, PB = Prudhoe Bay, FB = Franklin Bluff, U = Umiat, K = Kuparuk, and D = Mt. Doonerak. AA′ shows the endpoints of the modeled part of the TACT seismic line (Figure 13). BB′ shows the endpoints of a modeled line that encompasses an industry seismic line between CC′ (Figures 14–16). (b) Inset rectangle shows the map region spanned by Figures 4–8 and 10–12.

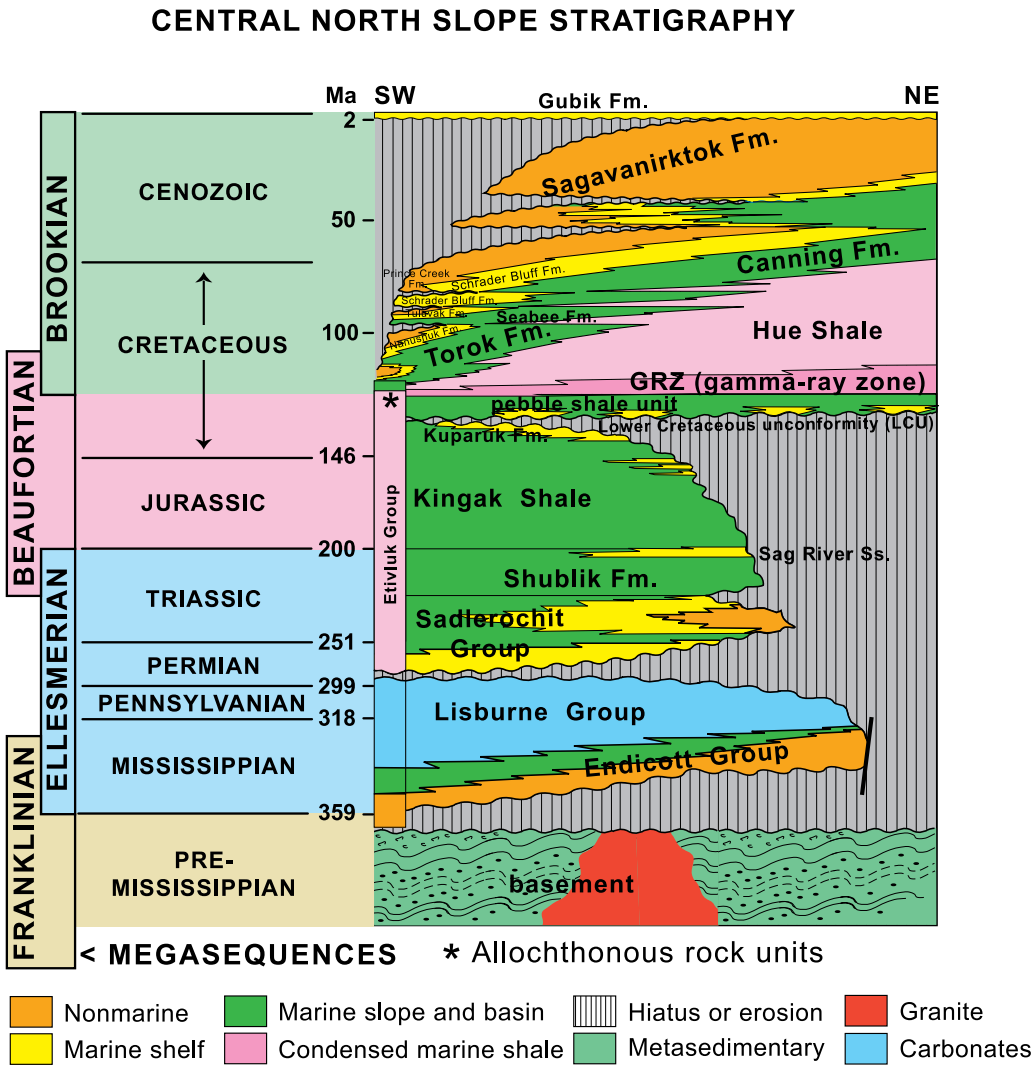

Figure 2. Generalized stratigraphy of the central North Slope, Alaska. Modified from Garrity et al. (2005).

particularly the southernmost part in the Brooks Range foothills.

Gravity and aeromagnetic data provide critical clues to both the deep and shallow structural framework of the relatively unexplored parts of the central North Slope. This geophysical framework provides constraints on the interpretation of regional structures and trends with implications for hydrocarbon exploration and evaluation. Where available, high-resolution gravity and aeromagnetic data also provide important clues to shallow structure, including possible targets for exploratory drilling.

In this article, we describe the gravity and aeromagnetic data for the central North Slope. Our focus is on the general interpretation of the data, with a look at deep structure and at shallow structural trends and the ways in which these interpretations complement and extend knowledge from drilling and regional seismic data. Finally, we outline general conclusions and make suggestions for further study.

REGIONAL GEOLOGY

Figure 2 provides the stratigraphic framework for the central North Slope. Figure 3 depicts the generalized geology. The Mississippian to Triassic Ellesmerian megasequence and its pre-Mississippian low-grade metamorphic basement (Franklinian megasequence) are considered to be part of a passive continental margin (south facing in present-day coordinates) on the northwestern edge of North America. This passive margin collided with an arc-related terrane in the latest Jurassic to the Early Cretaceous, leading to the initiation of the Brooks

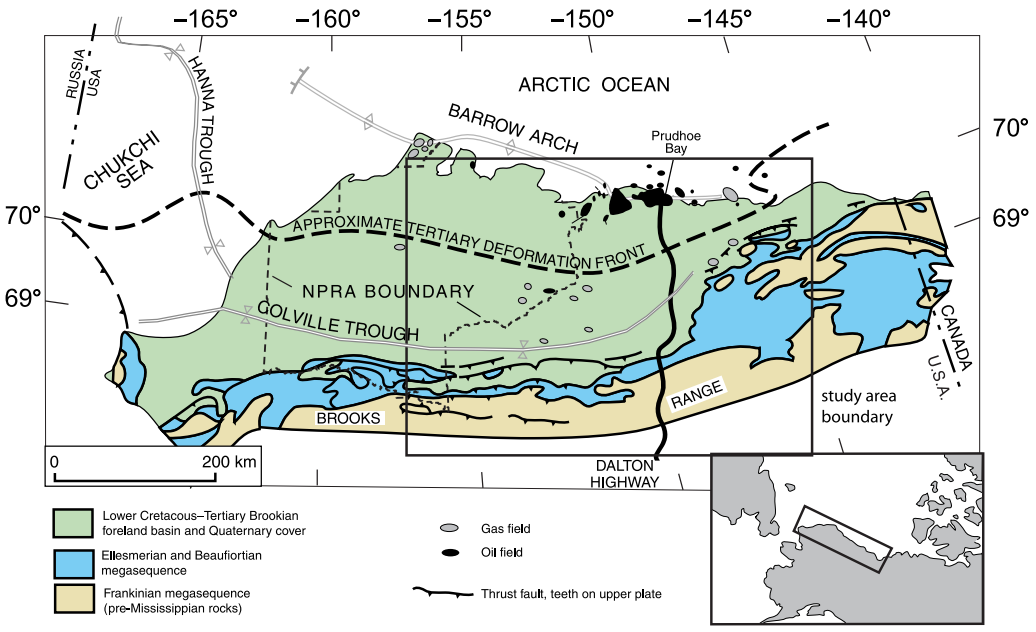

Figure 3. Generalized geology of Alaska's North Slope including location of primary oil and gas fields.

Range (Moore et al., 1994a). The Jurassic and Lower Cretaceous Beaufortian megasequence (Figures 2, 3) records incipient rifting related to the eventual middle Cretaceous opening of the Canada basin (Grantz et al., 1994). As a result of this ocean opening, the Arctic Alaska terrane, a fragment of the early North American margin, was left stranded in the location of the present-day North Slope (Moore et al., 1994a). The middle Cretaceous to Tertiary Brookian megasequence (Figures 2, 3) overlies the Pebble shale and the Lower Cretaceous unconformity (LCU) and consists of several northeastward-prograding, continental-margin sequences derived from the uplifted Brookian orogen; these sequences fill the foredeep north of the Brooks Range and step out across the north-facing Arctic passive margin (e.g., Saltus and Bird, 2003).

The foothills and the southern part of the Arctic coastal plain of the central North Slope contain the frontal part of a complex Tertiary fold-thrust belt. These Tertiary folds and thrusts are superimposed on the Middle Jurassic to Early Cretaceous main phase of deformation that affects the southernmost part of the foothills belt and the Brooks Range to the south. Both episodes of crustal shortening were dominantly north vergent.

Tertiary deformation across the central North Slope records a transition in structural style from thin skinned in the west to strongly basement involved in the east. West of the Dalton Highway, thrusting north of the Brooks Range front is fundamentally thin skinned. Geologic and geophysical data across that region indicate the presence of a thin-skinned triangle zone above a regional detachment in the Jurassic and Lower Cretaceous Kingak Shale (Figures 2, 3) underlying the foothills and a detachment-folded domain in Brookian Colville basin strata to the north. East of the Dalton Highway, the northeastern Brooks Range and the foothills to its north are characterized by thick-skinned, basement-involved thrusting, with a northward transition into thin-skinned thrusting and folding as deformation dies out at the front of the orogenic belt. The strong basement involvement continues eastward across the coastal plain in the ANWR (Grow et al., 1999; Moore, 1999; Potter et al., 1999, 2004; O'Sullivan and Wallace, 2002).

DESCRIPTION OF AVAILABLE GRAVITY AND AEROMAGNETIC DATA

Public-domain gravity data, much of it collected or compiled by Barnes (1976, 1977) and Barnes et al. (1994), are sparse in the central North Slope (Figure 4), consisting of several river traverses in the foothills, detailed data along the Dalton Highway and the nearby Trans-Alaska Crustal Transect (TACT) seismic profile, and scattered regional stations with a typical spacing of 20 km (12 mi). In contrast, within the NPRA, public-domain gravity data are available as a series of profiles along seismic lines with a typical spacing of 5 km (3.1 mi) or less. Along the profiles, the gravity station spacing ranges from about 100 to 500 m (330

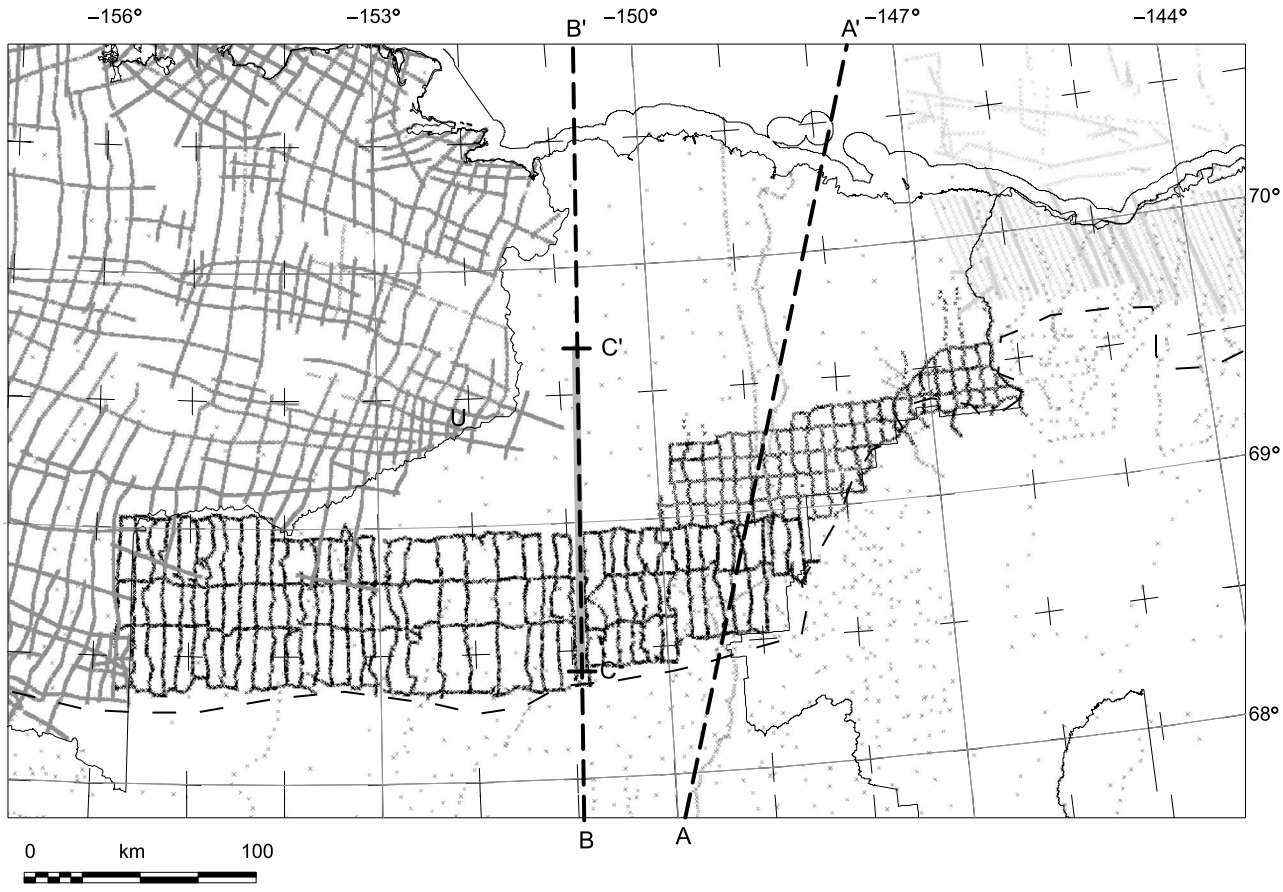

Figure 4. Gravity data index. Dark gray stations are part of the U.S. Geological Survey public-domain gravity data file. Black stations are proprietary data owned by PhotoGravity, Inc., Houston, Texas. Light-gray stations are ANWR data held by an oil company consortium. Dashed line profiles show the location of modeled cross sections. Base is from Figure 1.

to 1640 ft). Gravity data with similar spacing are available commercially for the foothills part of the central North Slope and for the ANWR coastal plain to the east (Figure 4).

A regional map of complete Bouguer gravity anomalies, prepared from the public-domain gravity data for the central North Slope, is shown in Figure 5. As expected for complete Bouguer gravity (i.e., Airy, 1855; Sleep and Fujita, 1997; Watts, 2001), the regional anomalies are inversely related to topography. Thus, the high topography of the Brooks Range coincides with low gravity values. In the lower elevations of the Arctic coastal plain, complete Bouguer gravity values are systematically higher than in the Brooks Range. The highest regional gravity values follow, in part, the basement high along the Barrow arch (Figures 3, 5). A local gravity low includes the location of the East Teshekpuk 1 drillhole that encountered granite in the shallow basement (Bird et al., 1978; Saltus et al., 2002).

Public-domain aeromagnetic data provide regional coverage for the central North Slope (Figure 6) and consist mostly of vintage data with 3.2-km (2-mi) flight-line spacing. These data include the 1945–1946 aeromagnetic survey of NPRA (Payne et al., 1952; Grauch and Castellanos, 1995), which is generally regarded as the first regional-scale aeromagnetic survey flown over land. These older data were collected with an analog system and have been digitized from compiled contour maps (Grauch and Castellanos, 1995; Connard et al., 1999). The southern part of the study area is spanned by digital flight-line data for aeromagnetic surveys conducted by the U.S. Geological Survey in 1976 (with 1.6-km [1-mi] flight-line spacing) and 1982 (3.2-km [2-mi] flight-line spacing). To the east, the coastal plain is spanned by a 1981 survey (Cunningham et al., 1987; Donovan et al., 1988) flown to investigate the possibility of direct aeromagnetic hydrocarbon detection. South of this survey, the only known aeromagnetic coverage is provided by regional reconnaissance profiles flown (with 16-km [10-mi] flight-line spacing) in 1965 and digitized from a regional compilation map. High-resolution commercial aeromagnetic data

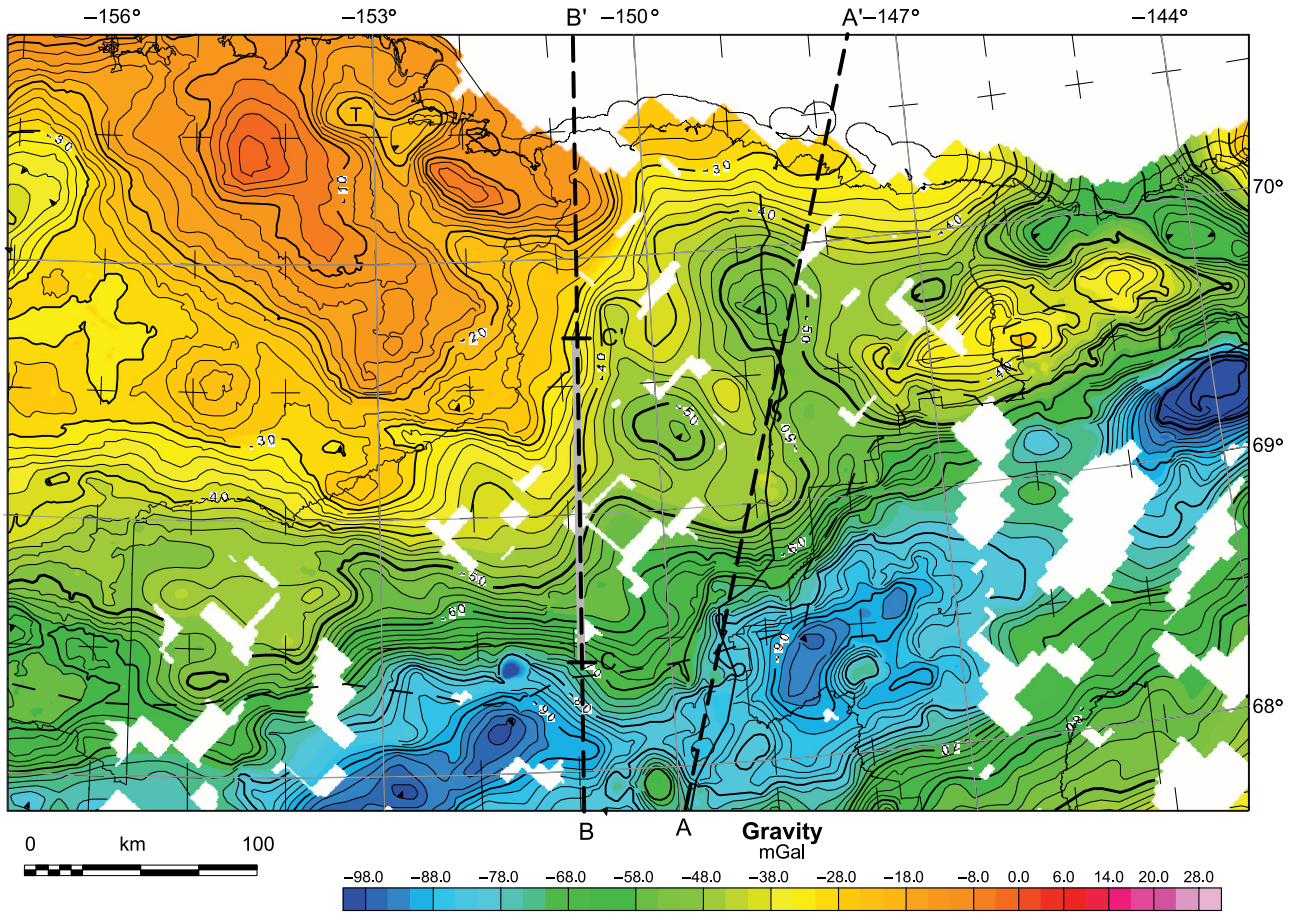

Figure 5. Regional gravity map. Complete Bouguer gravity anomalies from the U.S. Geological Survey public-domain data file. Contour interval 2 mGal. T = East Teshekpuk 1 drillhole. Heavy dashed line profiles show the location of modeled cross sections. Base map is from Figure 1.

(line spacing of 800 m [2600 ft] or less) have also been flown over parts of the central North Slope, including the ANWR 1002 (coastal plain) area and west into eastern NPRA. Additional, medium-resolution (typically 1.6-km [1-mi] spacing) aeromagnetic data are available commercially for other coastal regions of the North Slope.

A regional map of total field aeromagnetic data, corrected for the International Geomagnetic Reference Field (Figure 7), has been prepared from the public-domain data (Saltus and Simmons, 1997; Saltus et al., 1999a). The primary feature on this map is the long-wavelength, North Slope magnetic high in the western part of the central North Slope. This feature is caused by magnetic rocks that comprise a significant part of the pre-Mississippian basement, possibly mafic intrusions related to a (Devonian?) failed rift (Saltus et al., 1999b). Aside from the North Slope magnetic high, the regional magnetic field of northern Alaska, north of the Brooks Range, is regionally subdued, consistent with a nonmagnetic sedimentary section and a weakly magnetic basement. Several local magnetic highs, including two in the northern part of the central North Slope, may indicate upper crustal, magnetite-bearing intrusions. A northwest-southeast–trending aeromagnetic trough (labeled A in Figure 7) flanks the northeast boundary of the North Slope magnetic high. This feature indicates a zone of relatively nonmagnetic crustal rocks as well as suggesting a northwest-trending structural grain.

LONG-WAVELENGTH (DEEP) GEOPHYSICAL FEATURES

The broad magnetic anomalies of the 1945–1946 regional aeromagnetic survey of NPRA, and adjoining areas to the east, primarily reflect basement structure and composition (Figure 8). No data processing was performed to isolate the long-wavelength (deep-structure)

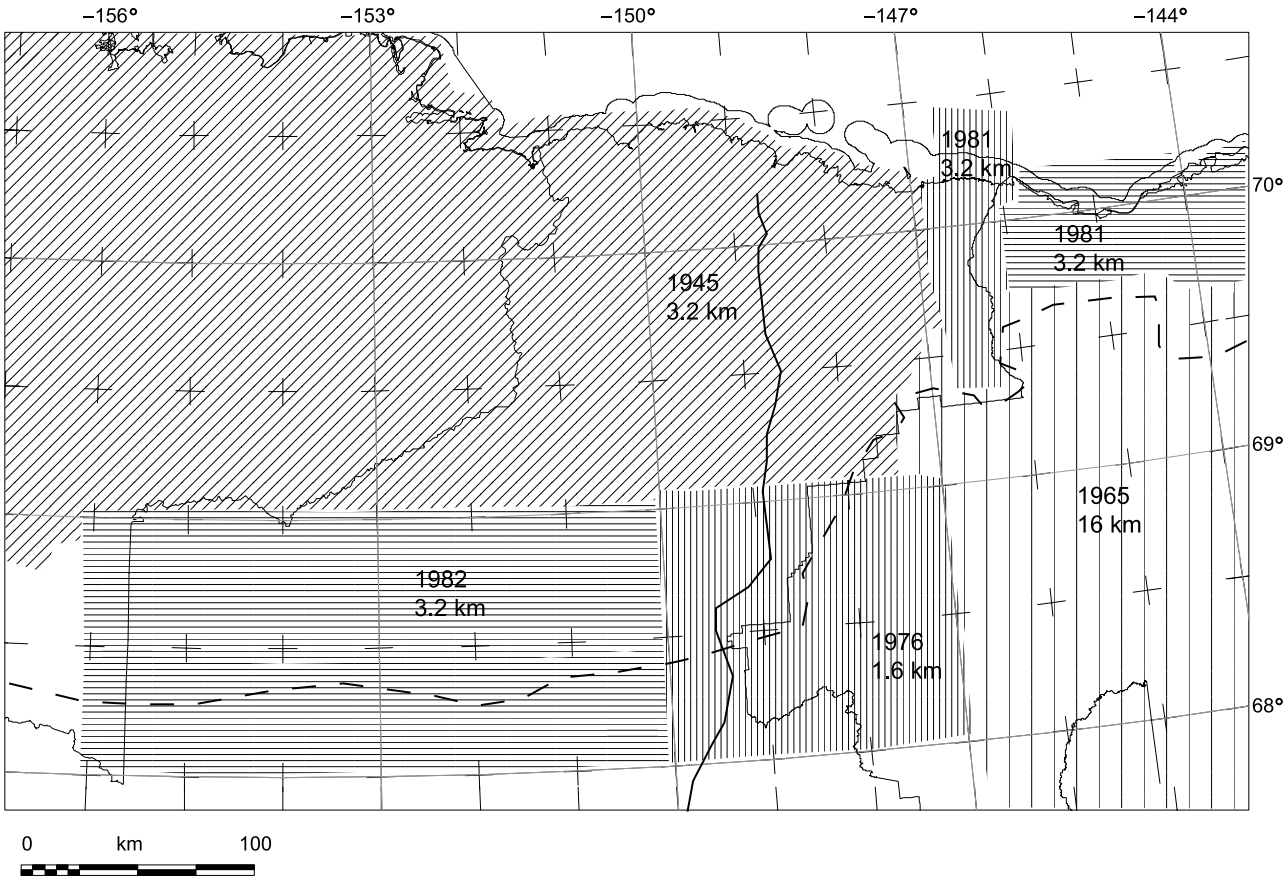

Figure 6. Aeromagnetic data index. Regional, public-domain, aeromagnetic surveys included in the statewide merged aeromagnetic grid (Saltus and Simmons, 1997) spanning the central North Slope. Direction of pattern lines indicates approximate direction of survey flight lines. Base is from Figure 1.

part of this data set in Figure 8; these long wavelengths are naturally dominant, especially in the historical part of the survey flown in 1945–1946. These wavelengths dominate because of the relative lack of shallow magnetic sources, the wide flight-line spacing, and the analog nature of the older survey. A detailed analysis of these data (Phillips et al., 2002; Saltus et al., 2002) does reveal a small number of low-amplitude features that represent magnetic sources (likely volcanic) in the post-Mississippian section, but these features are too subtle to see in Figure 8. In addition, by displaying the data as flat color bands in Figure 8, instead of employing shaded relief as in Figure 7, we further emphasize the long-wavelength features.

At the largest scale, we interpret two basement zones. The southwestern part of the central North Slope features a thick and highly magnetic basement zone that gives rise to part of the North Slope magnetic high (labeled A in Figure 8). This magnetic anomaly may reflect mafic and ultramafic rocks of a failed rift (Saltus et al., 1999b). The North Slope magnetic high terminates to the northeast along a northwest-southeast boundary. To the northeast of this boundary, the central North Slope basement has a generally neutral magnetic character punctuated by a nonmagnetic or reversely magnetized zone (anomaly B, Figure 8) and three discrete magnetic highs (C, D, and E, Figure 8). The nonmagnetic basement zone (B, Figure 8) could reflect nonmagnetic (or possibly reversely magnetized) sedimentary-protolith rocks in the crystalline basement. The northwest-southeast trend of this zone parallels the edge of the North Slope magnetic high and may be related structurally. The remaining magnetic highs (C–E, Figure 8) could reflect broad zones of igneous intrusion in a crystalline basement. All of these highs show bounding trends that are oriented northwest-southeast or northeast-southwest.

Numerous attempts have been made to analyze gravity data in NPRA. In particular, the problem of regional and residual separation for the purpose of isolating upper crustal anomalies has received much attention. Broadly following the work of Nunn et al. (1987)

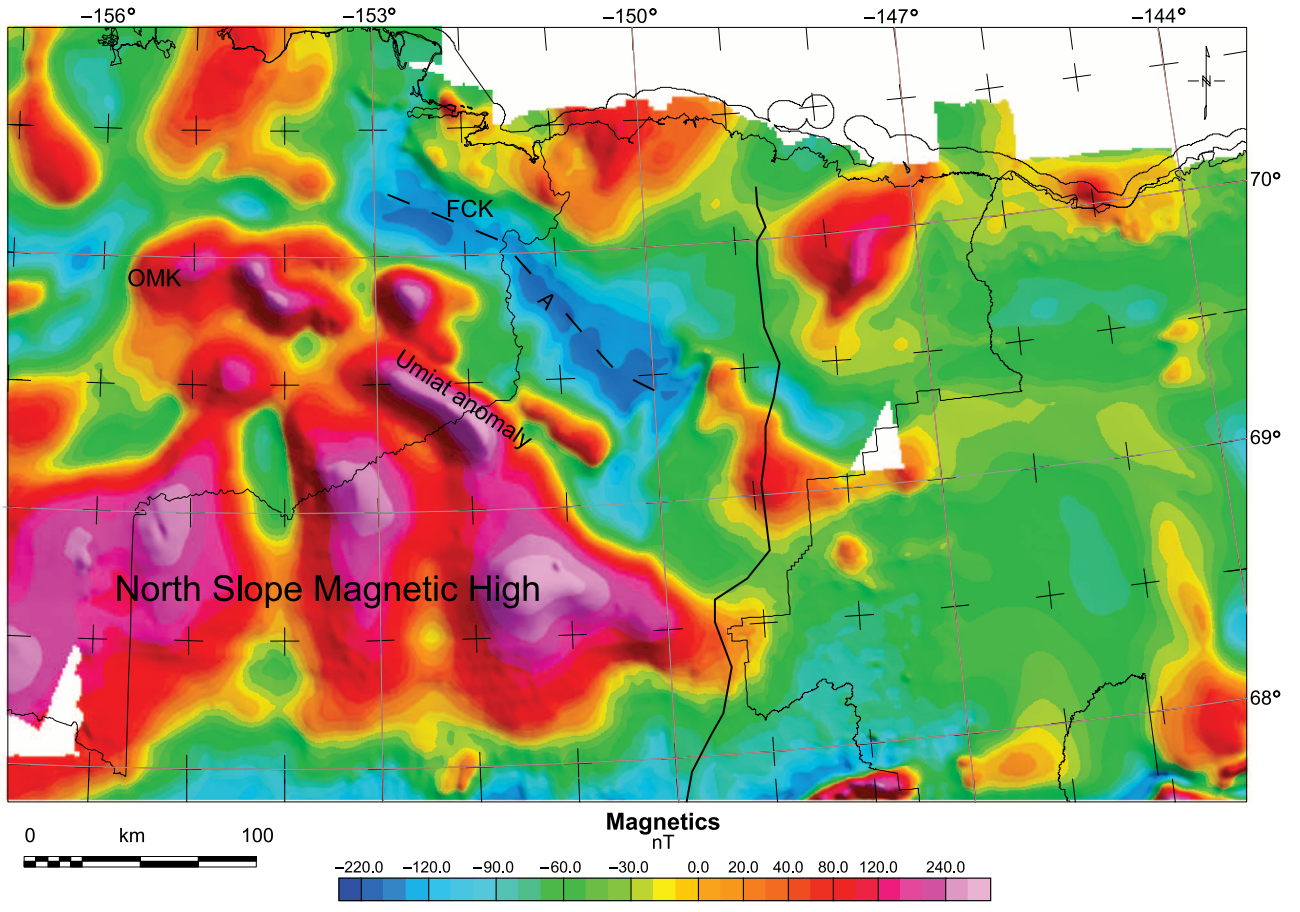

Figure 7. Regional aeromagnetic map. Subset of the Alaska statewide merged aeromagnetic map (Saltus and Simmons, 1997). OMK = Oumalik, FCK = Fish Creek. Dashed line and A mark magnetic trough discussed in the text.

and Spurlin (1993), we feel that it is appropriate to apply a gravity regional field based on regional isostasy and flexural rigidity of the crust. Insufficient independent constraints (i.e., no regional seismic mapping of the Moho) are available to produce a unique physical model for isostatic regional removal in northern Alaska. We have therefore developed an empirical, damped isostatic approach to regional and residual separation for the central North Slope. Instead of applying the full isostatic regional gravity field from a local Airy isostatic model, we multiply first by an appropriate fraction (damping factor) to produce a partial isostatic correction.

Comparative analysis of gravity and topography (Figure 9) can be thwarted if there is a significant correlation between topography and geology. On the North Slope, the Colville basin, containing a thick sedimentary section of lower density rocks, lies beneath the low topography of the coastal plain and northern foothills. In contrast, the Brooks Range correlates generally with exposures of rocks of higher density relative to the basin. To avoid this elevation and density bias, we performed our comparisons of gravity and topography only on regions with elevation in excess of 500 m (1640 ft). This eliminates the systematic correlation of low gravity and low elevation values of the Colville basin and coastal plain from the analysis.

The resulting residual gravity map (Figure 10) shows the upper crustal gravity anomalies that persist after the removal of a damped isostatic regional gravity field. We calculated the appropriate damping factor (in this case 0.782) by examination of the correlation of residual gravity and topography higher than 500 m (1640 ft) (Figure 9), for the North Slope, after application of the factor. Complete Bouguer anomalies are related to topography along a trend line with a slope of -30.3×10^{-3} mGal/m (Figure 9). Local (Airy, 1855; Simpson et al., 1986) isostatic anomalies show a correlation trend line of $+8.5 \times 10^{-3}$ mGal/m, consistent with the idea that flexural strength of the crust is preventing the full attainment of local isostatic equilibrium. If the local isostatic regional gravity field is multiplied

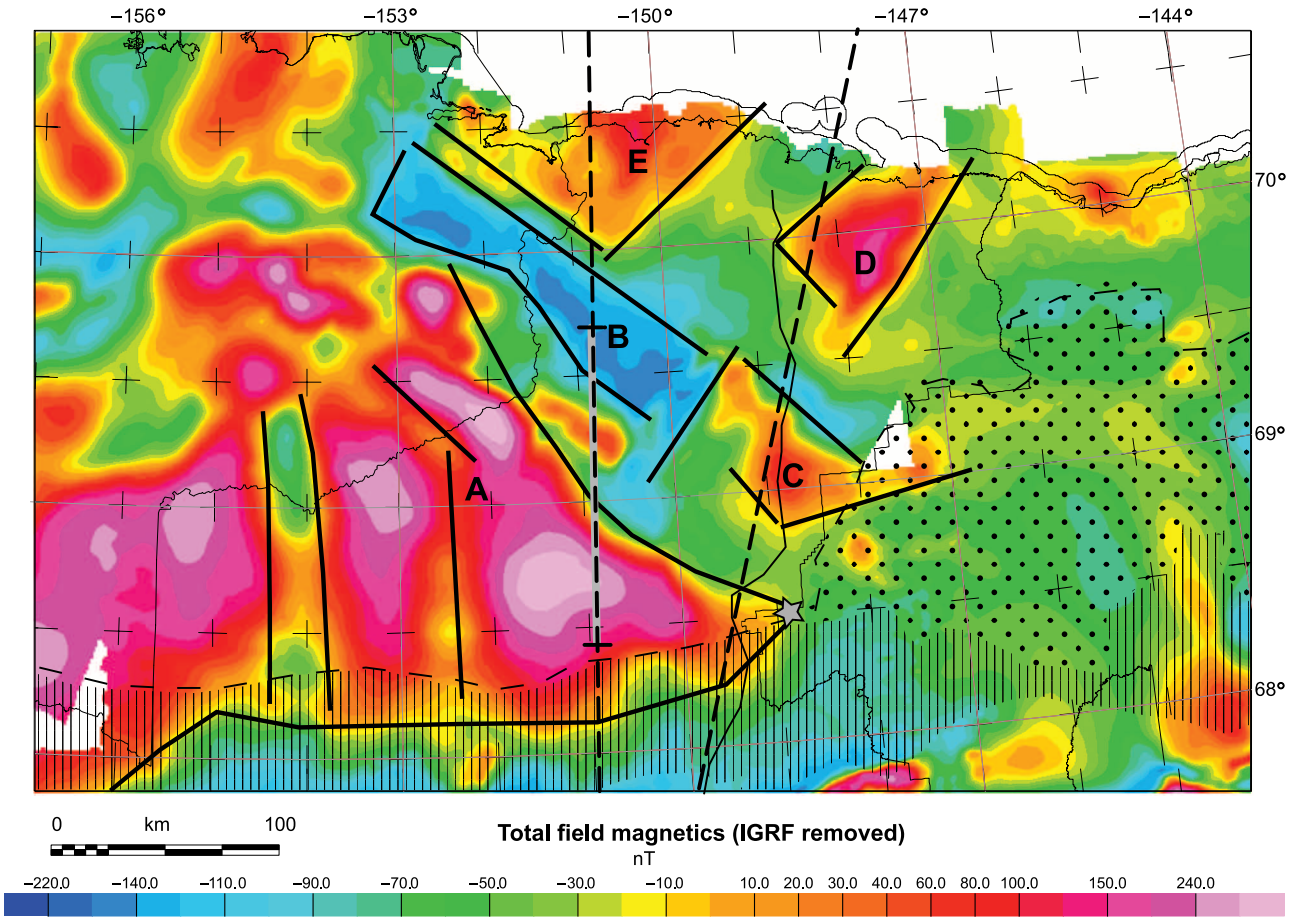

Figure 8. Long-wavelength (deep) magnetic map. Heavy lines denote magnetic boundaries and trends. Letters denote specific anomalies discussed in the text. The dot pattern marks the mapped extent of the North Slope subterrane (Moore et al., 1994b). The star marks the intersection of geologic and geophysical trends and a bend in the Brooks Range mountain front. The hachure pattern marks the mapped extent of the Endicott Mountains subterrane (Moore et al., 1994b). Dashed line profiles show the location of modeled cross sections. Base map is from Figure 1.

by a damping factor of 0.782 before subtraction from the complete Bouguer gravity, the resulting damped isostatic residual shows no statistical correlation of gravity and topography for regions of the North Slope with elevations greater than 500 m (1640 ft). This implies that about 20% of the support of Brooks Range topography results from the horizontally distributed flexural strength of the lithosphere. The remaining 80% of the support arises from isostatic buoyancy relating to the vertical distribution of lithospheric density.

The damped isostatic residual gravity anomalies for the central North Slope (Figure 10) reflect lateral variations in rock density from the surface into the mid-crust, including a significant part of the pre-Mississipian basement. As observed in previous gravity interpretations for northern Alaska, the residual gravity field does not show a simple relationship to upper crustal geology. In fact, the damped isostatic residual anomalies show a high degree of correlation with the basement features observed in the regional aeromagnetic data. Broadly speaking, the southwestern part of the central North Slope shows high gravity values (in general agreement with the location of the North Slope magnetic high). The northeastern part of the central North Slope shows low gravity values in the region of generally neutral aeromagnetic values. These broad trends do not mimic the isopachs of the Lower Cretaceous to Cenozoic Brookian sedimentary section (shown in Figure 10) (i.e., Saltus and Bird, 2003). The sedimentary section (Figure 2), as known from drilling and seismic data, thickens steadily from the Barrow arch southward to the northern foothills throughout the central North Slope and should, therefore, cause a gravity low to the south where the low-density sedimentary rocks are the thickest. If this basin gravity effect is modeled using the known basin configuration (e.g., Saltus and

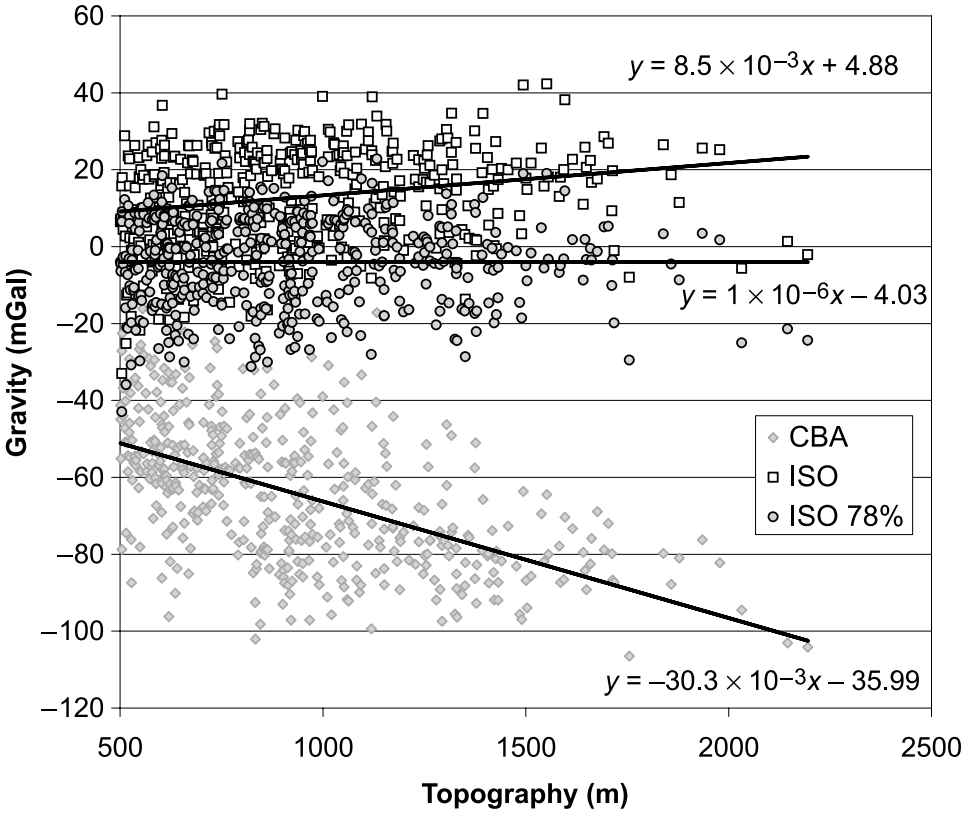

Figure 9. Correlation plot of gravity (mGal) versus topography (meters), North Slope, Alaska. CBA = complete Bouguer gravity anomaly; ISO = Airy isostatic residual gravity anomaly; ISO 78% = isostatic residual after subtraction of 78% of the calculated complete Airy isostatic gravity regional anomaly.

Bird, 2003) and then subtracted from the isostatic residual anomaly (as done in NPRA by Saltus et al., 2001), the resulting basement gravity map shows an even greater correlation with regional aeromagnetic anomalies.

The overall conclusion from examination of the long-wavelength components of the gravity and aeromagnetic data is that the central North Slope has two distinct basement zones that are separated by a northwest-southeast trend that crosses to the northwest into NPRA near the Umiat bend in the Colville River. To the southwest of this diagonal boundary (shown as a thick gray line in Figure 10), the basement rocks are generally dense and magnetic and may reflect a major crustal component of mafic, failed rift material. Regional geophysical trends in this southwest zone include northwest-southeast trends near the boundary, north-south trends farther south and west, and east trends at the southern margin. To the northeast of this diagonal boundary (Figure 10), the basement appears to be generally low density and magnetically neutral, reflecting a granitic or metasedimentary character. Regional geophysical trends in the northeastern basement zone are conjugate northwest-southeast and northeast-southwest (Figure 10).

SHORT-WAVELENGTH (SHALLOW) GEOPHYSICAL FEATURES

A shallow crustal structure is reflected in short-wavelength features of gravity and aeromagnetic data. The application of matched filters (Syberg, 1972; Phillips, 1997, 2001) provides a formal method for defining optimum Fourier-domain filters for the frequency slicing of gravity and magnetic data. The technique involves the visual identification of linear zones on a radially averaged power spectrum plot. Each of these trend lines is then converted into a band-pass filter. Finally, the individual filters are iteratively optimized so that they sum to match the observed spectrum. Because of the physical separation between shallow and deep anomaly sources, this technique is particularly effective for potential field data that span parts (Figures 11, 12) of the central North Slope.

Modern, high-resolution aeromagnetic data collected on the North Slope contain short-wavelength anomalies that are related to shallow folding and thrusting of the sedimentary section. In the Beaufort coastal plain in ANWR, these anomalies have been tied to shallow seismic interpretations and can be modeled as a direct consequence of folding, faulting, and erosional

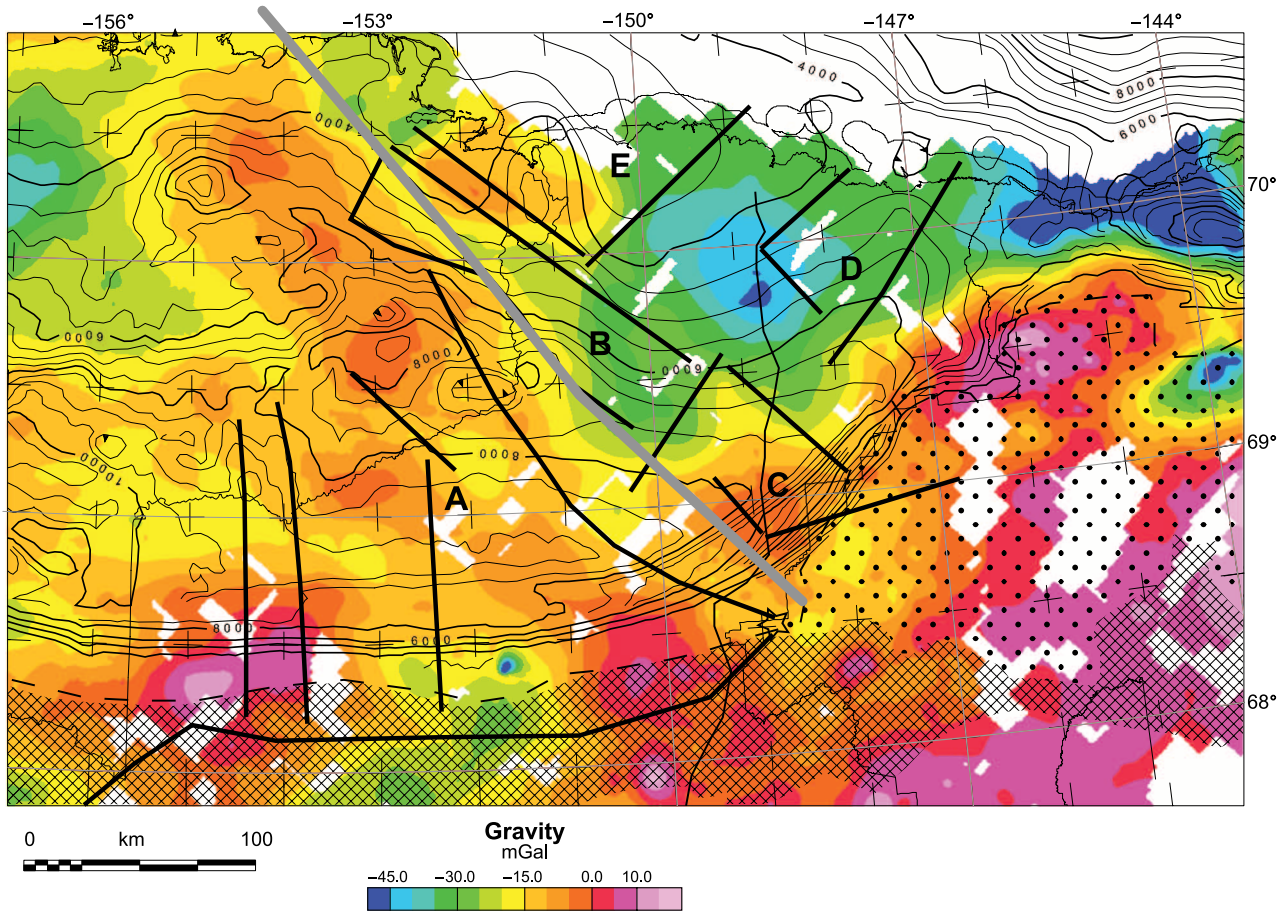

Figure 10. Damped isostatic residual gravity anomaly map. The gravity values show residual anomalies after a regional gravity field, based on flexural isostasy, is removed from complete Bouguer gravity anomaly data. Contour lines (interval 500 m [1640 ft]) are thickness of sedimentary section from Saltus and Bird (2003). Base map is from Figure 6. Black lines are basement boundaries and trends identified from the regional aeromagnetic data.

truncation of magnetic sedimentary layers in the Tertiary deltaic section (Phillips, 1999; Phillips et al., 1999; Potter et al., 2004). The observed magnetic anomalies can be reproduced with forward models consisting of magnetic layers that parallel the seismically determined shallow structure. The precise nature of the magnetization is unknown but may arise directly from detrital variations in the magnetic content of the deposited sediments or from chemical magnetization acquired as sediments accumulated (Phillips et al., 1999).

Similar short-wavelength aeromagnetic anomalies extend into and through the central North Slope (Figure 11). We infer that these features, as in the coastal plain in ANWR to the east, reflect disturbance of the shallow sedimentary section by folding and thrusting. The mapped magnetic patterns encompass a wider zone as one proceeds westward. The width of this trend is governed, at least in part, by the much broader north-south extent of Brookian sedimentary rocks to the west, where the Brooks Range front lies much farther south.

In the central North Slope region, two general zones of short-wavelength magnetic anomalies are present. The first is a narrow zone to the north where lower Tertiary rocks are exposed at the surface (e.g., Franklin Bluffs; Mull et al., 2003b) with a northwest-southeast strike. This zone lies above the northeastern geophysical basement domain. The second is a broader east-west zone to the south (but still well north of the Brooks Range mountain front; this zone lies above the southwestern geophysical basement domain) where mostly Upper Cretaceous rocks are exposed at the surface (Mull et al., 2004). The western part of the southern anomaly zone (box labeled A in Figure 11) includes a northwesterly set of features. The split between these anomaly zones may further broaden into NPRA, where high-resolution aeromagnetic data are presently unavailable. We expect the southern band of shallow

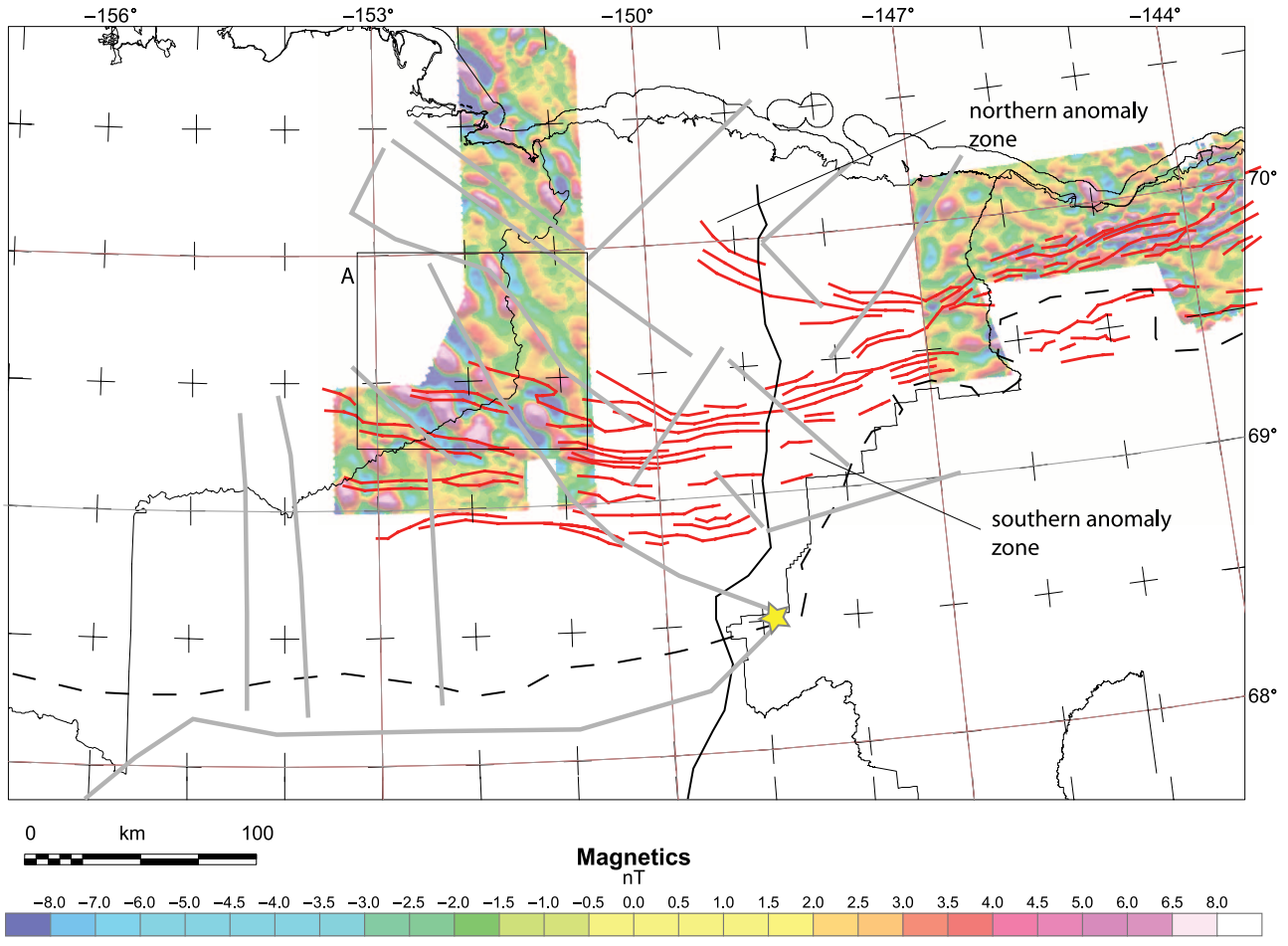

Figure 11. Short-wavelength (shallow) magnetic map. Color-shaded regions are band-pass-filtered versions of a part of the high-resolution, proprietary aeromagnetic data available from Fugro Geosurveys, Inc. (used with permission from Fugro Airborne Surveys). Red lines show shallow aeromagnetic features identified from the proprietary aeromagnetic data (Fugro Geosurveys, Inc.; used with permission). Gray lines are basement boundaries and trends identified from the regional aeromagnetic data. The box labeled A contains anomaly trends discussed in the text. Base is from Figure 1.

aeromagnetic features to swing into a north-south trend parallel to the western updip limit of the Upper Cretaceous Seabee Formation as shown on the NPRA geologic map of Mayfield et al. (1988).

Public-domain gravity data for the central North Slope are too widely spaced to map shallow structural features. Proprietary gravity data span the foothills region in a 75-km (46-mi)-wide belt extending north of the Brooks Range mountain front (Figure 4). These data, collected on north-south transects with an average spacing of about 8 km (5 mi), can be gridded using a bidirectional algorithm and then match filtered (Syberg, 1972; Phillips, 1997, 2001) to highlight features with wavelengths of a few kilometers (Figure 12). Although not quite as detailed, the public-domain gravity data spanning NPRA, when processed in a similar fashion, reveal fine-scale features as well (Figure 12).

Several discrete, short-wavelength, linear gravity features can be identified on the filtered gravity map (Figure 12). In the northeastern part of the data area, several short linear features (features 1–3 in Figure 12) can be identified with an east-west trend and average spacing of about 10 km (6 mi). Feature 1 corresponds to the Kavik structure, on which the undeveloped Kavik gas field is located (Verma et al., 2005). To the south, a band of four linear features (4–7 in Figure 12) trend in a more southwesterly direction, with an average spacing of about 10 km (6 mi). Gravity feature 4 appears to be a composite of two geologic structures, based on seismic reflection interpretation and surface geology. The eastern part of feature 4 corresponds to a basement-involved fold at the mountain front (possibly continuous with the Echooka anticlinorium of Meigs and Imm, 1995), and the western part of feature 4 corresponds

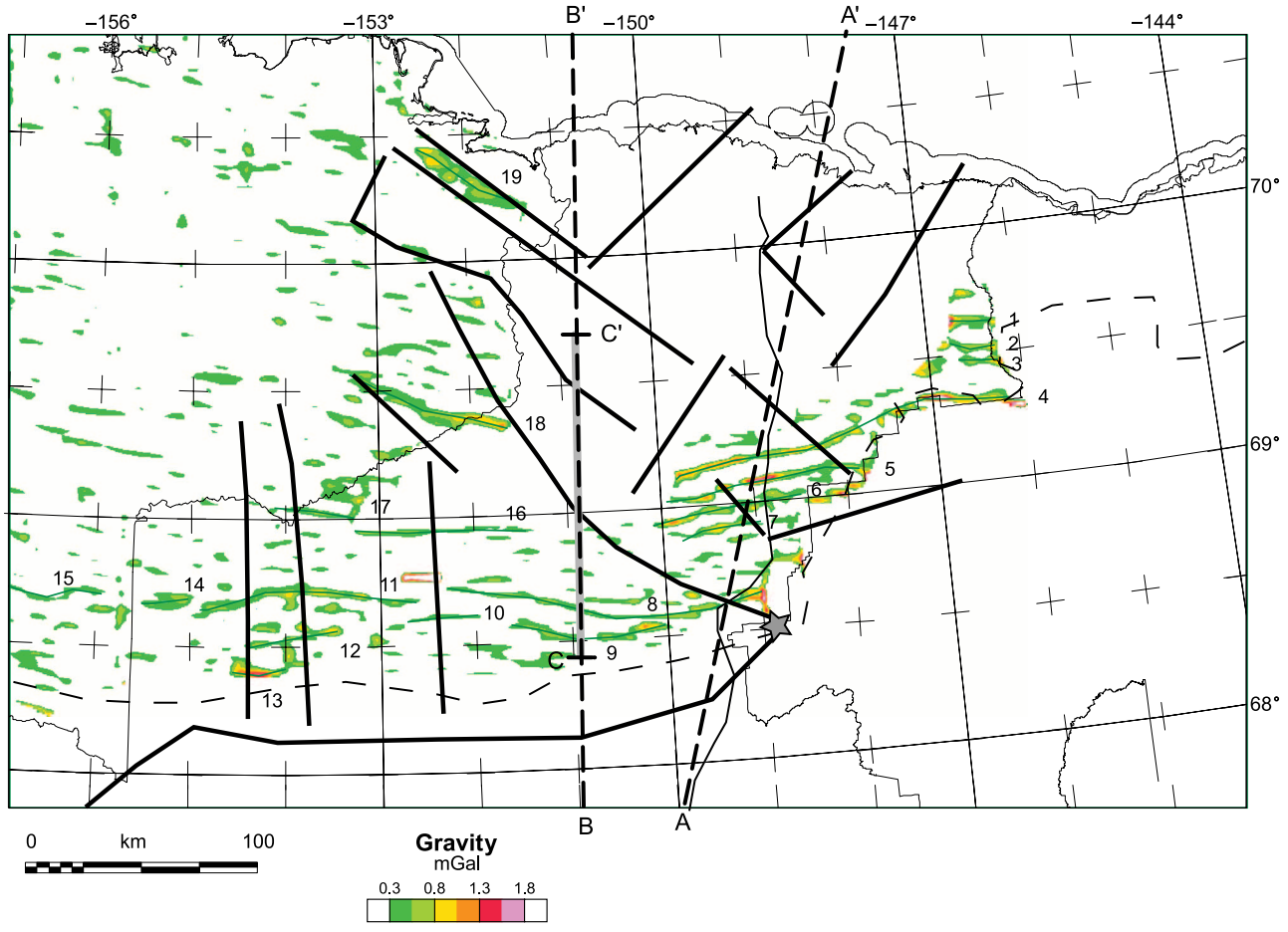

Figure 12. Short-wavelength (shallow) gravity map. Colored areas indicate gravity highs on a high-pass-filtered gravity map, constructed using bidirectional gridding, from U.S. Geological Survey public-domain gravity data in NPRA and PhotoGravity proprietary gravity data east of the Colville River. The numbered features are discussed in the text. Black lines represent basement boundaries and trends identified from regional aeromagnetic data. Dashed line profiles show the location of modeled cross sections. Base is from Figure 1.

to a prominent thrust-related anticline developed in the Brookian section (with only minor basement involvement) and tested by the Aufeis well. Gravity features 5–7 also correspond to anticlines interpreted from proprietary seismic reflection data, with slightly less confidence, as regional two-dimensional (2-D) seismic lines are of poorer quality in the foothills. Continuing farther south, an east-west zone, about 30 km (18 mi) wide, contains no continuous linear gravity features. South of this trend-free zone is a fairly continuous, curvilinear set of more or less east-west–trending linear gravity features (features 8, 11, 14, and 15 in Figure 12) that extend westward into NPRA. In general, this area is poorly imaged on proprietary seismic data, but these trends seem reasonable as expressions of foothill structural trends as discussed in the next section. Feature 8 corresponds to the Tuktu escarpment, the southern limit of exposures of thick Lower Cretaceous sandstones. Features 11, 14, and 15 track an outcrop belt of Fortress Mountain Formation sandstones. Farther south is a second, less conspicuous set of curvilinear features (9, 10, and 12 in Figure 12). The eastern part of feature 9 corresponds to a belt of exposures of thrust-imbricated Lower Cretaceous Cobblestone sandstone (Mull et al., 2003a). Feature 13 corresponds to exposures of allochthonous mafic rocks in the Kikiktak Mountain klippe of Mull et al. (1994). An east-west gravity high (feature 16 in Figure 12) appears to correlate to the Grandstand anticline of Kelley (1990). Several linear features extend westward into NPRA (17–19 in Figure 12) with a more northerly trend to the west. Feature 18 is the Umiat anticline. These detailed geological correlations with high-resolution gravity anomalies demonstrate the utility of the gravity

method in this structurally complex region. We feel that further interpretation of existing high-resolution gravity as well as continued data collection will provide useful guidance to detailed structural studies and exploration in the Brooks Range foothills.

DETAILED INTERPRETATION ALONG TWO SEISMIC LINES

The TACT deep refraction seismic profile follows the Dalton Highway across the central North Slope (Figure 1) (Fuis et al., 1995, 1997). Within our study area, complete Bouguer anomaly (CBA) gravity values (Figures 5, 13) along the TACT are broadly antithetic to topography, with low gravity values coincident with the high Brooks Range and neutral gravity values along the coastal plain. Total field magnetic values (Figures 8, 13) along this part of the TACT are relatively subdued. The TACT skirts around the edge of the North Slope magnetic high (labeled A in Figure 8) and crosses a smaller magnetic high (C in Figure 8) and part of a third magnetic high (D in Figure 8).

A 2-D forward model (Figure 13) shows a broad physical property framework that is consistent with the seismic results and the potential field data. The model honors the block and layer boundaries identified by Fuis et al. (1997). Densities were initially set based on conversion from refraction velocities (Fuis et al., 1997) using the relations of Gardner et al. (1974) and Jones (1996) and then adjusted incrementally to obtain a reasonable fit to the data. The regional (CBA) gravity low is caused by the position of the Moho, which reaches a depth of about 48 km (30 mi). The deeper slab, identified based on seismic refraction (Fuis' layer 10, Figure 13), is indistinguishable from the mantle (layer 11) in its gravity expression. Upper crustal densities in this model are consistent with a crystalline and dense carbonate composition for the pre-Brookian rocks exposed in the Brooks Range and with lower density sedimentary rocks in the Colville basin.

The lower crust (Fuis' layer 9, Figure 13) requires considerable heterogeneity in physical properties (both density and magnetic susceptibility) to match the observed gravity and magnetic data. The details of this physical property variation are not uniquely determined by this model, but the scale of the variation shows that it is significant. Three basement regions (labeled A, B, and C on panel 3 of Figure 13) with elevated magnetic susceptibility are required to explain the three magnetic highs crossed by the TACT. Magnetic susceptibilities of between 25 and 27 mSI (equivalent to a magnetic intensity of about 1.2 A/m) were assigned to these bodies. These magnetic values are consistent with a range of intrusive rock types from intermediate to mafic in composition. Each of these anomalous basement regions also represents density heterogeneity in this model. The northern basement body (C, panel 3, Figure 13) requires a significantly lower density than the surrounding basement to match the local gravity low (see also Figure 10). This may represent a region of felsic composition (although with sufficient magnetite to be significantly magnetic).

Inferred seismic velocities and interpreted basement lithologies along the TACT profile (Fuis et al., 1997) do not significantly reflect the presence of a dense body in the basement required by the gravity and aeromagnetic data in the vicinity of the Brooks Range mountain front (the North Slope magnetic high, A in Figure 8). We attribute this discrepancy to the fact that the TACT profile just clips the eastern limit of the geophysical features. Seismic energy from these features would be expected to have a significant three-dimensional component; it would not necessarily be well imaged in 2-D seismic data. In addition, gravity and aeromagnetic data were not incorporated in the seismic interpretation (Fuis et al., 1997).

Although commercial detailed gravity (Figure 4) and aeromagnetic data (Figure 11) are available for parts of the TACT (Figure 4), the seismic refraction interpretation (Fuis et al, 1997) is not sufficiently detailed to constrain shallow interpretation. That aspect of potential field interpretation is better illustrated in our next geophysical cross section.

Industry reflection seismic lines have been collected in the southern part of the central North Slope. We will examine one line that is available to the U.S. Geological Survey and is used here with permission from WesternGeco (Figure 14, location shown in Figure 1). A regional gravity and magnetic model, analogous to the TACT model (Figure 13), shows that the crustal root beneath the high Brooks Range topography is primarily responsible for the long-wavelength gravity low centered roughly on the high topography. The general shape of the Colville basin in this model is based on a compilation (Saltus and Bird, 2003) of regional seismic and drillhole data. The gravity low caused by sedimentary rocks in the basin is offset in the model by the high densities in the pre-Mississippian basement (model body with density of 2810 kg/m^3). This same dense body is also magnetic and accounts for the broad aeromagnetic anomalies along this line (part of the North Slope deep magnetic high). The style of the

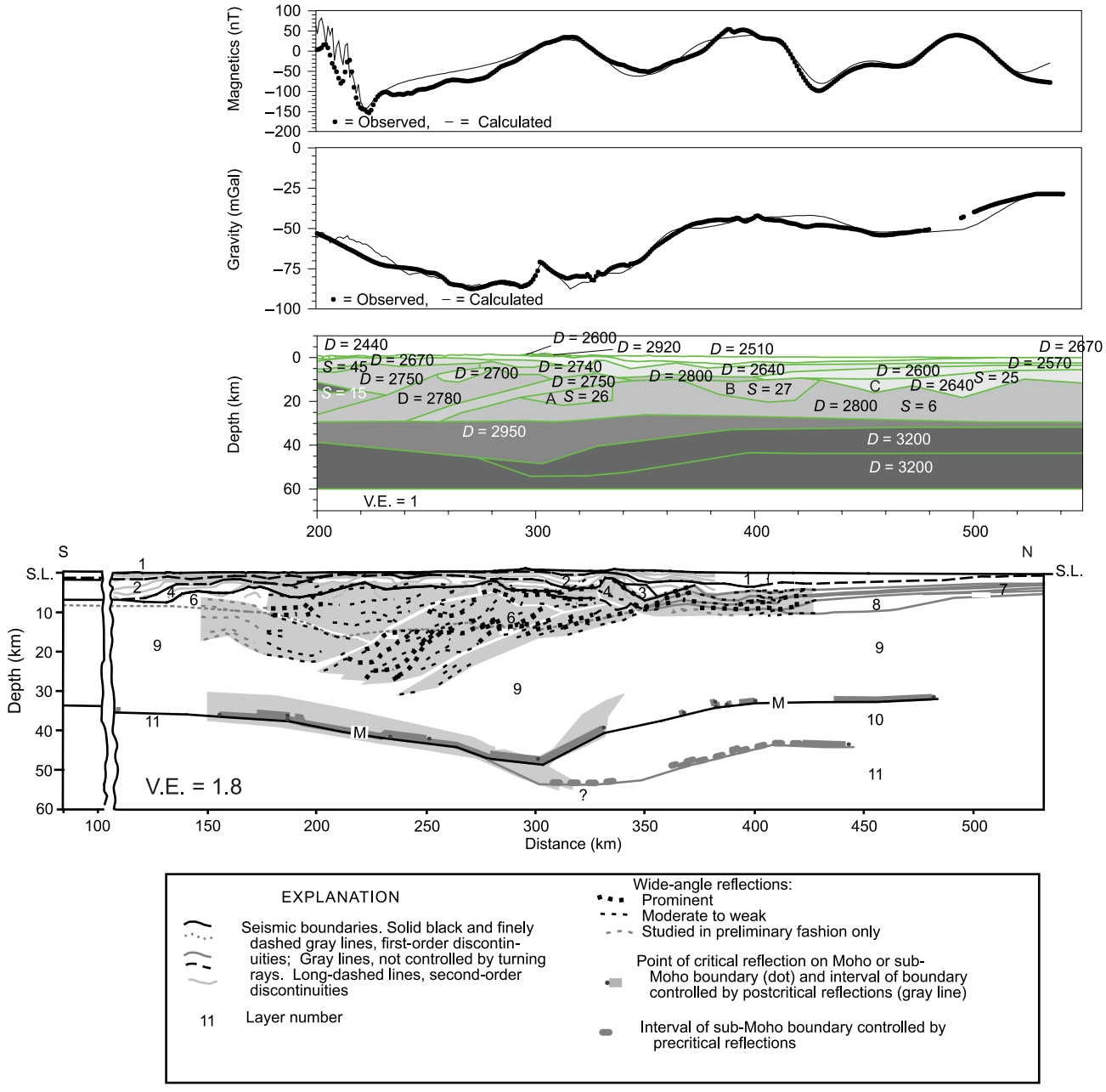

Figure 13. Geophysical cross section interpretation along the Trans-Alaska Crustal Transect (TACT; location shown in Figure 1 and many subsequent figures as AA′). The top panel depicts observed (dots) and calculated (line) magnetic anomalies. The second panel depicts observed (dots) and calculated (line) gravity anomalies. The third panel shows the cross sectional geophysical block model with densities (*D*) labeled in kg/m^3 and magnetic susceptibilities (*S*) labeled in mSI. M = Moho. Calculated anomalies shown in panels one and two arise from the two-dimensional (infinite in and out of the frame) bodies shown in panel 3. Panels 4 and 5 are from Fuis et al. (1997) and depict and explain the refraction seismic interpretation for the TACT. The geophysical model was built to (1) honor the crustal blocks defined in the seismic interpretation of Fuis et al. (1997); (2) contain densities consistent with seismic velocities (Fuis et al., 1997) with only minor adjustment; and (3) match the broad aeromagnetic anomalies with high-susceptibility and high-density bodies in the pre-Mississippian basement.

gravity model at the southern end of the line (south of the Colville basin) is based generally on the structural style of the TACT line seismic interpretation (Figure 13) (Fuis et al., 1997).

The interpretation shown on the seismic line (Figure 14) is generalized. Three stratigraphic horizons are picked: the top of the pre-Mississippian basement, the top of the Triassic Shublik Formation, and

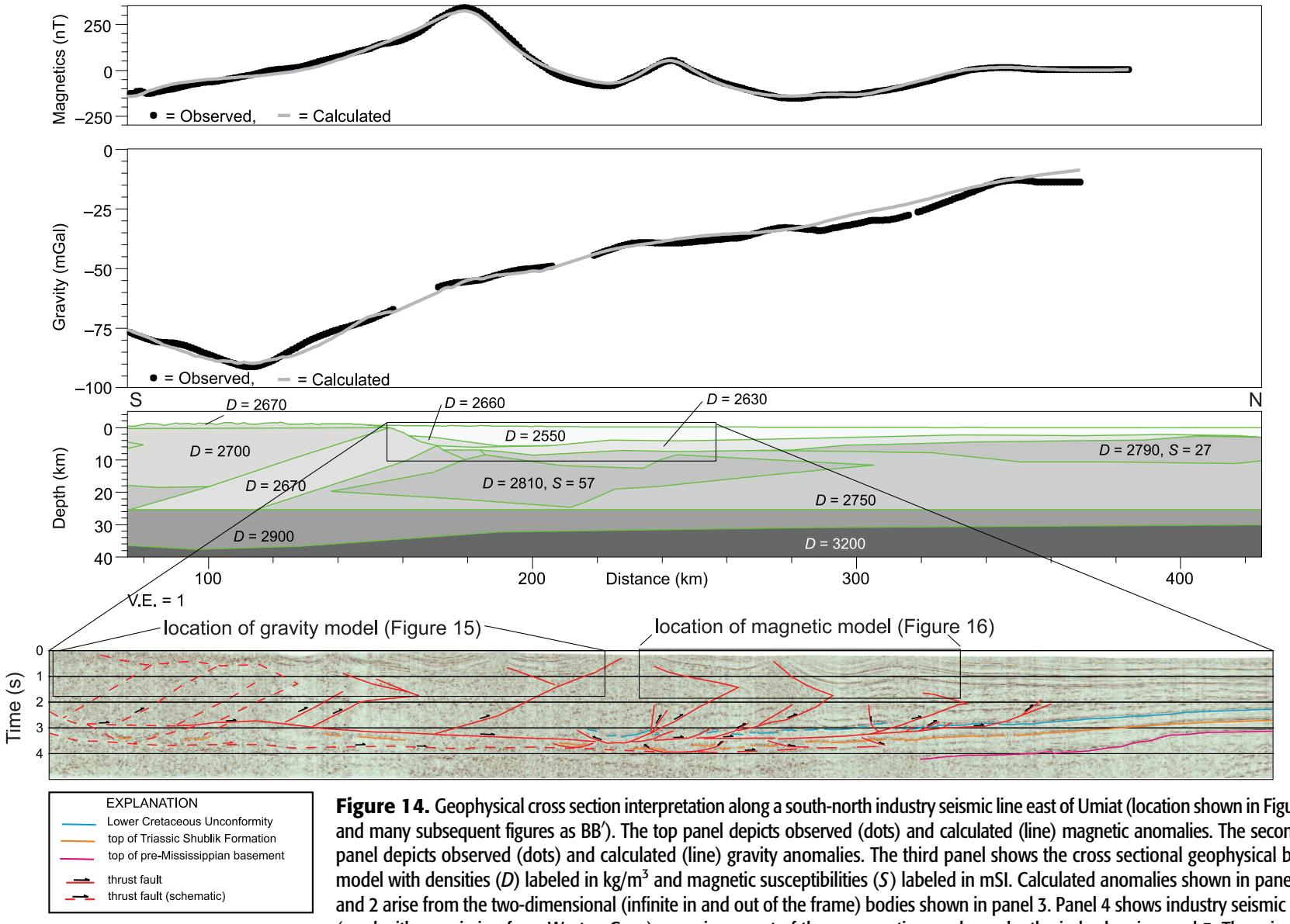

Figure 14. Geophysical cross section interpretation along a south-north industry seismic line east of Umiat (location shown in Figure 1 and many subsequent figures as BB′). The top panel depicts observed (dots) and calculated (line) magnetic anomalies. The second panel depicts observed (dots) and calculated (line) gravity anomalies. The third panel shows the cross sectional geophysical block model with densities (*D*) labeled in kg/m^3 and magnetic susceptibilities (*S*) labeled in mSI. Calculated anomalies shown in panels 1 and 2 arise from the two-dimensional (infinite in and out of the frame) bodies shown in panel 3. Panel 4 shows industry seismic data (used with permission from WesternGeco) spanning a part of the cross section as shown by the index box in panel 3. The seismic interpretation lines depict the general structural style and show the top of pre-Mississippian basement, the top of the Triassic Shublik Formation, and the Lower Cretaceous unconformity. The geophysical model was built to (1) follow the general style of crustal blocks defined in Figure 13 and (2) match the broad aeromagnetic anomalies with high-magnetic-susceptibility and high-magnetic-density bodies in the pre-Mississippian basement.

the LCU (Figure 2). The structural interpretation illustrates several fundamental elements of the thrust structure of the Brooks Range foothills and southern coastal plain. In this frontal part of the Brookian orogen, the basal detachment steps up from the Triassic Shublik Formation to the Jurassic–Lower Cretaceous Kingak Shale and, ultimately, into the Lower Cretaceous to Paleogene part of the Brookian megasequence. The southern part of the interpretation, shown with dashed lines, is a generalized portrayal of the tip of a large passive-roof duplex (triangle zone), which likely corresponds to the area of poor seismic data quality at the south end of the line. To the north, the basal detachment locally ramps up into the Brookian section, where structural thickening and backthrusting underlie prominent anticlines in the fold belt at the front of the deformation belt.

High-pass filtering of high-resolution gravity data (Figure 12; used with permission from PhotoGravity) reveal four small-amplitude (less-than-1-mGal) gravity highs along the southernmost part of the seismic line spaced at intervals between 12 and 15 km (7.5 and 9.3 mi) (Figure 15). The middle two highs were discussed previously (gravity highs labeled 8 and 9 in Figure 12). Two density interfaces contribute to the model. The first is the contrast in density between surficial rocks (modeled here as 2600 kg/m^3) and the gravity reduction density of 2670 kg/m^3. This effect leads to gravity lows over hills and highs over valleys. Superimposed on this effect is a second modeled density contrast with denser (2670-kg/m^3) rocks at shallow depths. The shape of this second density contrast surface is based generally on the shallow continuation of anticlinal and synclinal patterns observed in the shallow seismic data in the northern part of this line segment (Figure 15). Note that the specific densities chosen for this model are ad hoc; the model is meant to illustrate the general nature of the gravity sources. In detail, the density structure is undoubtedly more complex. The model shows two anticlinal culminations in the southern part of the seismic line where coherent reflectors are lacking. These two structural highs correspond to the Arc Mountain anticline and the Cobblestone culmination (Mull et al., 2003a). Our conclusion is that the high-pass gravity highs in this region can be used to map structural highs that occur within the upper 1 km (0.6 mi) or so of the subsurface.

High-resolution aeromagnetic data are available (proprietary data owned by Fugro, Inc. and displayed here with permission) for the northern part of this seismic line (Figures 11, 16). Subtle features (amplitudes of only ±5 nT for a flight height of 500 ft [152 m]) can be reasonably modeled as the effect of magnetic stratigraphy in the shallow rock section (Figure 16). This general model is analogous to models of high-resolution aeromagnetic data in the Beaufort coastal plain of the ANWR (Phillips et al., 1999), but differs from these models in one key aspect: we are not including reversely magnetized layers for which there is, as yet, no physical property evidence. If the surrounding rocks have a sufficiently high magnetization (here, a magnetization of 1.0 mSI is the nominal background shown in the deep part of the model), then stratigraphic intervals with lower-than-background magnetization will cause relative magnetic lows without the need to invoke reverse remanent magnetization in the model.

Depending on the magnetic stratigraphy, the association of magnetic features to geologic structure may be complex. In this model, the local magnetic highs are related to the truncation of relatively magnetic layers at or near the surface. A prominent local magnetic low (at a distance of 94 km [58 mi] along the profile) is interpreted as a very weakly magnetized zone in the crest of an anticlinal fold. This zone lacks coherent reflectors in the seismic line, perhaps indicating the disruption of the stratigraphy by faulting. The weak magnetization zone could be the result of alteration or leaching of magnetic minerals in this faulted zone or erosion of the magnetic layer that is present on the flanks of the anticline.

DISCUSSION

The function of basement structures in the evolution of continental regions has been widely recognized and discussed (e.g., Holdsworth et al., 1998, 2001; Sims et al., 2005). Central North Slope basement domains and trends correlate, in many cases, with mapped and inferred shallow structures and structural trends. This suggests a causal relationship between the deep and shallow structures. We postulate that deep geophysical boundaries represent zones of stress concentration that have influenced the reaction of the Arctic Alaska plate to tectonic events. The reactivation of deep structures may help explain the regional patterns of uplift and erosion mapped by Burns et al. (2002).

Whether thick-skinned (basement-involved) or thin-skinned thrusting occurs in a compressional tectonic setting is largely dependent on the overall strength profile of the crust (e.g., Babeyko and Sobolev, 2006). Although the basement-involved nature and the Tertiary age of deformation in the northeastern Brooks

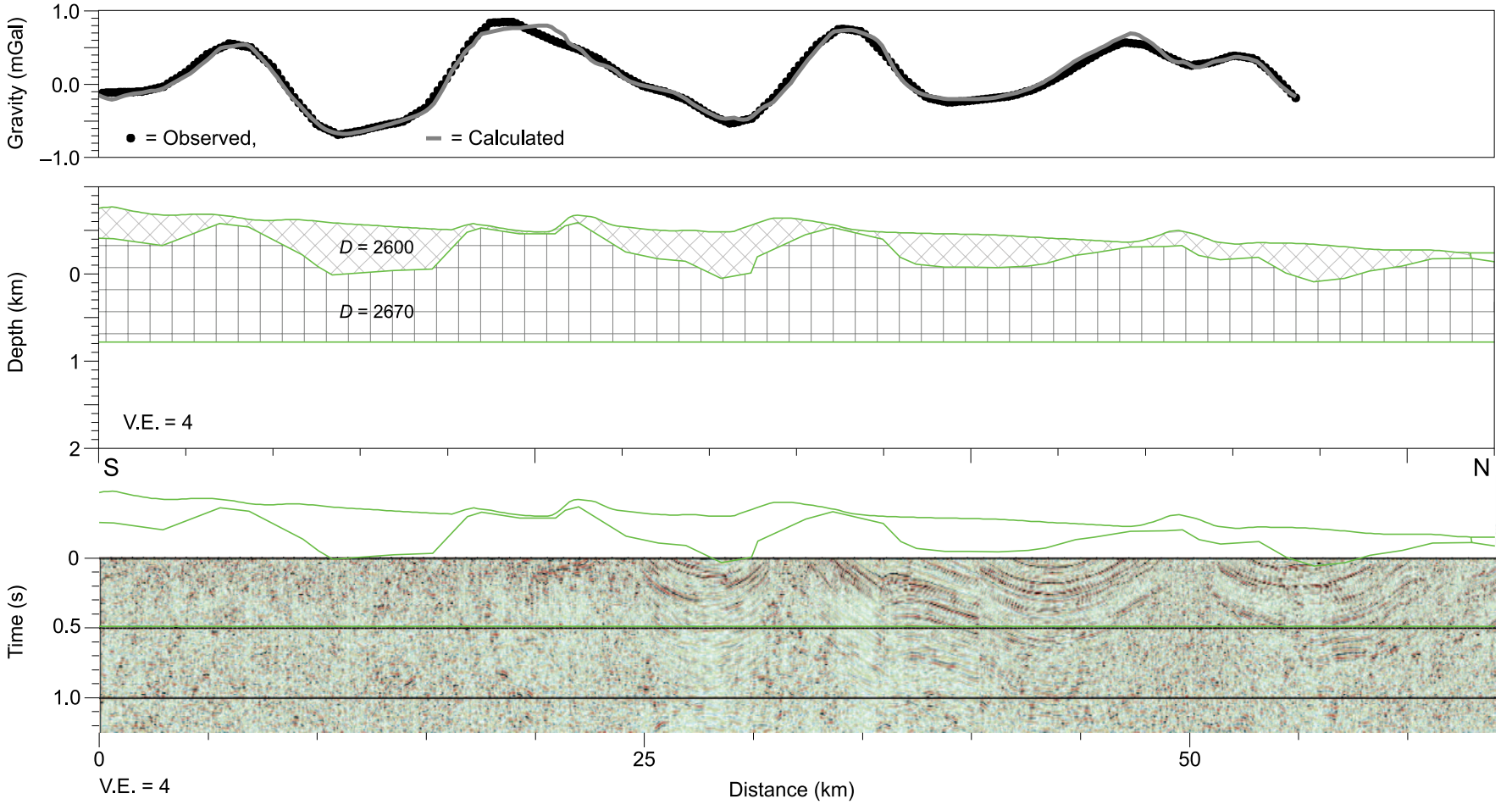

Figure 15. Interpretation of high-pass-filtered, high-resolution gravity data along a part of the WesternGeco seismic line east of Umiat (used with permission from WesternGeco) (see Figure 14). The top panel depicts observed (dots) and calculated (line) gravity anomalies. The second panel shows the cross sectional geophysical block model with densities (*D*) labeled in kg/m^3. Calculated anomalies shown in panel 1 arise from the two-dimensional (infinite in and out of the frame) bodies shown in panel 2. Panel 3 shows the location of the geophysical model in relation to a part of the seismic line (full line displayed in Figure 14).

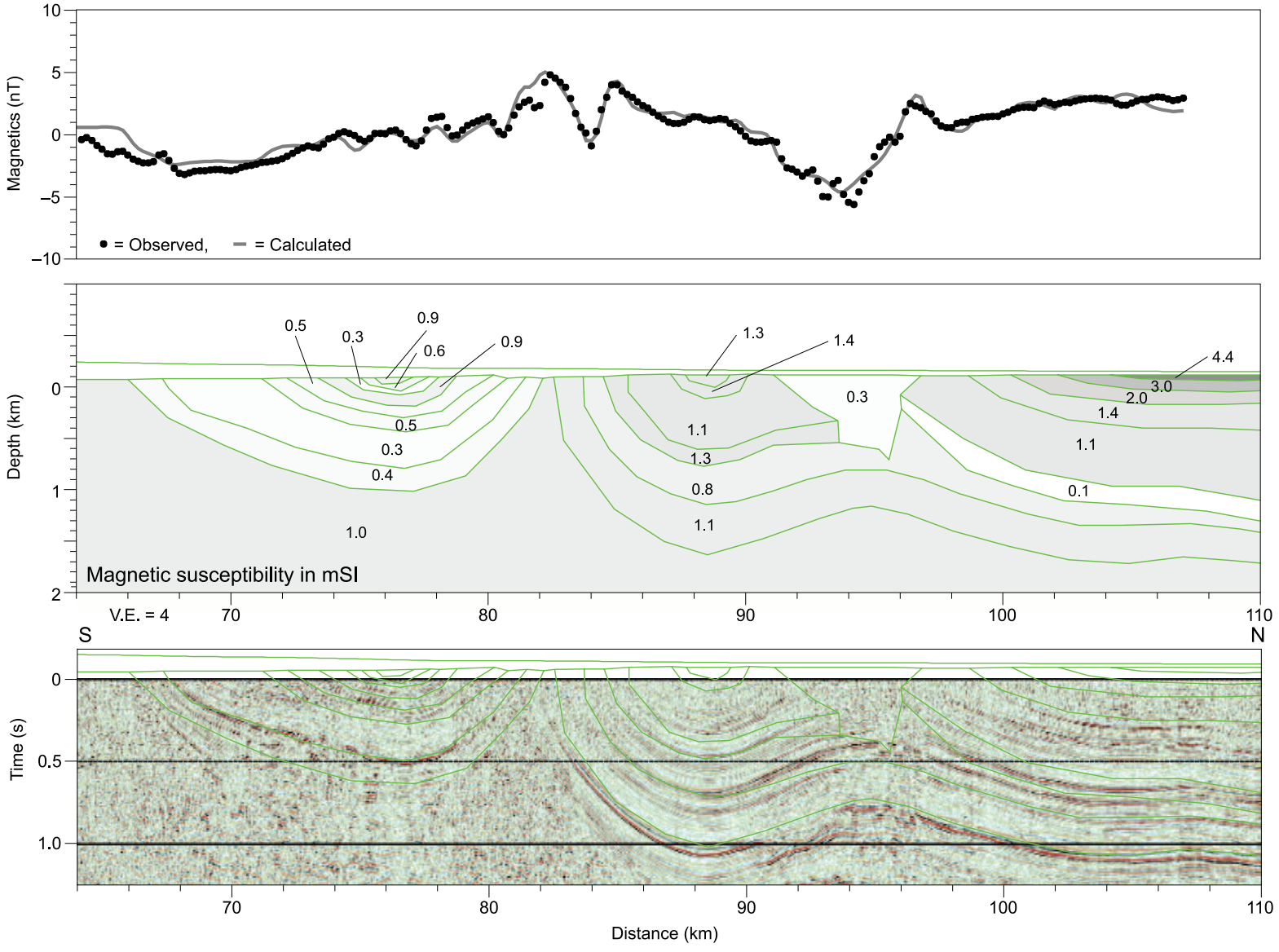

Figure 16. Interpretation of high-pass-filtered aeromagnetic data along a part of the WesternGeco industry seismic line east of Umiat (used with permission from WesternGeco) (see Figure 14 for location). The top panel depicts observed (dots) and calculated (line) magnetic anomalies. The second panel shows the cross sectional geophysical block model with magnetic susceptibilities labeled in mSI. Calculated anomalies shown in panel 1 arise from the two-dimensional (infinite in and out of the frame) bodies shown in panel 2. Panel 3 shows the location of the geophysical model in relation to a part of the seismic line (full line displayed in Figure 14).

Range were likely far-field expressions of stresses produced by plate convergence in southern Alaska (Moore et al., 1985; Grantz et al., 1994), lateral variations in the strength of the basement likely influenced the structural patterns in the shallow crust. In particular, the southern and eastern margins of the geophysical basement zone defined by the North Slope magnetic high coincide spatially with structural transitions and trends.

The southern boundary of the North Slope magnetic high lies north of the northern limit of thick-skinned, basement-involved thrusting as defined by seismic (Fuis et al., 1997) and structural (Moore et al., 1997) interpretations of the TACT and other seismic lines (Figures 13, 14). The eastern limit of the North Slope magnetic high, near the Atigun Gorge, correlates with the northward bend in the trend of the central Brooks Range mountain front (location in Figure 1). We propose that the dense, magnetic basement domain associated with the North Slope magnetic high represents a Devonian(?) failed rift and is dominated by mafic intrusions likely flanked by a weaker cogenetic sedimentary section. The mechanical strength and probable lack of stratification in this proposed mafic basement make it highly competent, forming a buttress against which the western Brooks Range was thrusted, so that thrusting farther north steps up into the sedimentary section and does not involve the basement rocks. To the east of the Atigun Gorge, where we infer a more silicic, metasedimentary basement, the basement-involved thrusting continues well to the north.

The Atigun Gorge also marks the approximate intersection of the boundary between the Endicott Mountains and North Slope subterranes with the northern front of the Brooks Range (Figures 3, 8) (Moore et al., 1994b). This is a faulted boundary between adjacent subterranes with distinct stratigraphies that imply significant relative displacement (Moore et al., 1994b). To the west of the Atigun Gorge, the subterrane boundary falls a few tens of kilometers north of the Brooks Range mountain front. To the east, the mountain front extends to more than 100 km (62 mi) north of the subterrane boundary. Exposures of pre-Mississippian rocks in the northeastern Brooks Range are complex and diverse (Moore et al., 1994b) and include rocks with both continental and oceanic affinity. A lower Paleozoic oceanic assemblage that includes mafic volcanic rocks in the basement exposed in the Romanzof Mountains (Dutro, 1981; Moore et al., 1994b) is of particular note as a possible surface analog for dense and magnetic basement rocks. These rocks were deformed during the Middle to Late Devonian (Anderson and Wallace, 1990) and may be analogous to the source rocks for the North Slope magnetic high.

In the western North Slope, aeromagnetic and gravity data are sparse. However, regional compilations (North American Magnetic Anomaly Group, 2002; Klemperer et al., 2002) suggest that the North Slope magnetic high may connect to the geophysical anomaly underlying the Hanna Trough, a major tectonic element in the Chukchi Sea (Figure 3). If so, this would support a connection, as hypothesized by Sherwood et al. (2002), between the Devonian and later rifting of the Hanna Trough and tectonic events associated with the Ellesmerian depositional sequence beneath the North Slope.

In summary, regional gravity and aeromagnetic data, publicly available for much of the North Slope of Alaska, reveal important information about fundamental basement composition and structural grain. The basement features may represent zones of weakness or stress concentration that have had a fundamental influence on both large- and small-scale tectonic development of the Brooks Range and the fold and thrust belt of northern Alaska. The whole crust geophysical property models illustrated by the cross section interpretations in Figures 13 and 14 provide a framework for a detailed analysis along other seismic lines or transects of interest throughout the North Slope.

Modern gravity and aeromagnetic surveys contain short-wavelength information absent in the older data and can be mathematically filtered, using readily available techniques and software, to highlight shallow features and trends. Shallow geophysical feature maps, particularly when linked to detailed seismic interpretations, are an important contribution to an integrated structural model of this complex area. The models presented in this article may provide useful guidelines for application elsewhere in the Brooks Range foothills belt.

Challenges for future geophysical work on the North Slope include (1) the collection of detailed, high-resolution aeromagnetic and gravity data spanning the entire North Slope; (2) the collection of regional deep-seismic soundings to map the Moho and upper mantle; (3) the integration and use of existing regional seismic information to construct a three-dimensional framework of the primary seismic horizons and the use of this model to analyze the intermediate wavelengths present in the gravity and aeromagnetic data; (4) better integration of gravity and magnetic data with seismic interpretation in depth; and (5) drilling of one or more deep scientific boreholes into the geophysical basement anomalies.

CONCLUSIONS

Regional aeromagnetic data for the North Slope show broad, high-amplitude anomalies that are related primarily to physical property variation in the pre-Mississippian basement. The understanding of regional gravity anomalies is more complex and requires a model of isostasy, constraints from deep seismic interpretation, and independent knowledge (from seismic and drilling) of the structure of the Colville basin. Taken together, these potential field constraints yield a geophysical model that demonstrates significant physical property heterogeneity in the pre-Mississippian basement. The combined geophysical model of the North Slope crust provides a template for regional and residual separation that should be of use to continued geophysical (particularly gravity) analysis and exploration in the region. Basement composition and structural trends appear to have had a major influence on both large- and small-scale tectonic development of the Brooks Range as well as the fold and thrust belt. The resistance of the dense and magnetic source of the North Slope magnetic high to basement deformation may have influenced the nature and location of basement-involved thrusting of the Brooks Range in northern Alaska. High-resolution gravity and aeromagnetic data contain short-wavelength features that can be used to map shallow structures and trends. Detailed models of short-wavelength gravity and aeromagnetic anomalies along a selected industry seismic line are models for the application of both new and existing high-resolution potential field surveys to future exploration.

REFERENCES CITED

Airy, G. B., 1855, On the computation of the effect of the attraction of the mountain-masses, as disturbing the apparent astronomical latitude of stations in geodetic surveys: Philosophical Transactions of the Royal Society of London, v. 145, p. 101–104.

Anderson, A. V., and W. K. Wallace, 1990, Middle Devonian to lower Mississippian clastic depositional cycles southwest of Bathtub Ridge, northeastern Brooks Range, Alaska: Geological Association of Canada–Mineralogical Association of Canada Program with Abstracts, v. 15, p. A2.

Babeyko, A. Y., and S. V. Sobolev, 2006, Quantifying different modes of the late Cenozoic shortening in the central Andes: Geology, v. 33, no. 8, p. 621–624.

Barnes, D. F., 1976, Bouguer gravity map of Alaska: U.S. Geological Survey Open-File report 76-70, scale 1:2,500,000, 1 sheet with interpretive text.

Barnes, D. F., 1977, Bouguer gravity map of Alaska: U.S. Geological Survey Map GP-913, scale 1:2,500,000, 1 sheet.

Barnes, D. F., J. Mariano, R. L. Morin, C. W. Roberts, and R. C. Jachens, 1994, Incomplete isostatic gravity map of Alaska, *in* G. Plafker and H. C. Berg, eds., The geology of Alaska: Geological Society of America, The Geology of North America, v. G-1, plate 9, scale 1:2,500,000, 1 sheet.

Bird, K. J., C. L. Connor, I. L. Tailleur, M. L. Silberman, and J. L. Christie, 1978, Granite on the Barrow arch, northeast NPRA, *in* K. M. Johnson, ed., The United States Geological Survey in Alaska: Accomplishments during 1977: U.S. Geological Survey Circular 772-B, p. B24–B25.

Burns, W. M., D. O. Hayba, D. W. Houseknecht, and E. L. Rowan, 2002, Timing of hydrocarbon generation in the National Petroleum Reserve–Alaska (NPRA) from burial and thermal history modeling: AAPG Bulletin, v. 86, no. 6, p. 1139.

Connard, G. G., R. W. Saltus, P. L. Hill, L. Carlson, and B. Milicevic, 1999, Alaska digital aeromagnetic database description: U.S. Geological Survey Open-File Report 99-0503, http://pubs.usgs.gov/of/1999/ofr-99-0503 (accessed April 15, 2006).

Cunningham, K. I., A. A. Roberts, and T. J. Donovan, 1987, Horizontal-gradient magnetic and helium surveys, *in* K. J. Bird and L. B. Magoon, eds., Petroleum geology of the northern part of the Arctic National Wildlife Refuge, northeastern Alaska: U.S. Geological Survey Bulletin, v. 1778, p. 209–218.

Donovan, T. J., J. D. Hendricks, A. A. Roberts, and P. T. Eliason, 1988, Low-level aeromagnetic surveying for petroleum in Arctic Alaska, *in* G. Gryc, ed., Geology and exploration of the National Petroleum Reserve in Alaska, 1974 to 1982: U.S. Geological Survey Professional Paper 1399, p. 623–632.

Dutro, J. T. Jr., 1981, Geology of Alaska bordering the Arctic Ocean, *in* A. E. M. Nairn, M. Churkin, Jr., and F. G. Stehli, eds., The ocean basins and margins: The Arctic Ocean: New York, Plenum Press, v. 5, p. 21–36.

Fuis, G. S., A. R. Levander, W. J. Lutter, E. S. Wissinger, T. E. Moore, and N. K. Christensen, 1995, Seismic images of the Brooks Range, Arctic Alaska, reveal crustal-scale duplexing: Geology, v. 23, no. 1, p. 65–68.

Fuis, G. S., J. M. Murphy, W. J. Lutter, T. E. Moore, and K. J. Bird, 1997, Deep seismic structure and tectonics of northern Alaska: Crustal-scale duplexing with deformation extending into the upper mantle: Journal of Geophysical Research, v. 102, no. B9, p. 20,873–20,896.

Gardner, G. H. F., L. W. Gardner, and A. R. Gregory, 1974, Formation velocity and density— The diagnostic basics for stratigraphic traps: Geophysics, v. 39, p. 770–780.

Garrity, C. P., D. W. Houseknecht, K. J. Bird, C. J. Potter, T. E. Moore, P. H. Nelson, and C. J. Schenk, 2005, U.S. Geological Survey 2005 oil and gas resource assessment of the central North Slope, Alaska: Play maps and results: U.S. Geological Survey Open-File Report 2005-1182, http://pubs.usgs.gov/of/2005/1182/2005-1182.pdf (accessed April 15, 2006).

Grantz, A., S. D. May, and P. E. Hart, 1994, Geology of the Arctic continental margin of Alaska, *in* G. Plafker and H. C. Berg, eds., The geology of Alaska: Geological Society of America, The Geology of North America, v. G-1, p. 17–48.

Grauch, V. J. S., and E. Castellanos, 1995, Revised digital aeromagnetic data for areas in and adjacent to the National Petroleum Reserve Area (NPRA), North Slope, Alaska: U.S. Geological Survey Open-File Report 95-0835, 11 p.

Grow, J. A., C. J. Potter, W. J. Perry, M. W. Lee, and M. Killgore, 1999, Structural framework and lithologic composition of the Niguanak high and the Aurora dome— Chapter NA (Niguanak and Aurora structures), *in* ANWR Assessment Team, The oil and gas resource potential of the 1002 Area, Arctic National Wildlife Refuge, Alaska: U.S. Geological Survey Open-File Report 98-34, CD-ROM, p. NA-1–NA-46.

Holdsworth, R. E., R. A. Strachan, and J. F. Dewey, 1998, eds.,

Continental transpressional and transtensional tectonics: Geological Society (London) Special Publication 135, 359 p.
Holdsworth, R. E., M. Stewart, J. Imber, and R. A. Strachan, 2001, The structure and rhyologic evolution of reactivated fault zones— A review and case study: Geological Society (London) Special Publication 184, p. 115–137.
Jones, G. W., 1996, Lower crustal density estimation using the density-slowness relationship— A preliminary study: M.S. thesis, Texas A&M University, College Station, Texas, 62 p.
Kelley, J. S., 1990, Generalized geologic map of the Chandler Lake quadrangle, north-central Alaska: U.S. Geological Survey Miscellaneous Field Studies, Map MF-2144-A, scale 1:250,000, 1 sheet, 19 p.
Klemperer, S. L., M. L. Greninger, and W. J. Nokleberg, 2002, Geographic information systems compilation of geophysical, geologic, and tectonic data for the Bering Shelf, Chukchi Sea, Arctic margin, and adjacent landmasses, *in* E. L. Miller, A. Grantz, and S. L. Klemperor, eds., Tectonic evolution of the Bering Shelf–Chukchi Sea–Arctic margin and adjacent landmasses: Geological Society of America Special Paper 360, p. 359–374.
Mayfield, C. F., I. L. Tailleur, and I. Ellersieck, 1988, Bedrock geologic map of the National Petroleum Reserve in Alaska, *in* G. Gryc, ed., Geology and exploration of the National Petroleum Reserve in Alaska, 1974 to 1982: U.S. Geological Survey Professional Paper 1399, p. 187–190.
Meigs, A. J., and T. A. Imm, 1995, Geometry and deformation of a duplex and its roof layer: Observations from the Echooka anticlinorium, northeastern Brooks Range, Alaska, *in* R. A. Combellick and F. Tannian, eds., Short notes on Alaska geology 1995: Alaska Division of Geological and Geophysical Surveys Professional Report 117C, p. 19–31.
Moore, T. E., 1999, Balanced cross section, Bathtub syncline to Beaufort Sea through Niguanak structural high, Arctic National Wildlife Refuge (ANWR), northeastern Alaska— Chapter BC (balanced cross section), *in* ANWR Assessment Team, The oil and gas resource potential of the 1002 Area, Arctic National Wildlife Refuge, Alaska: U.S. Geological Survey Open-File Report 98-34, CD-ROM, p. BC-1–BC-61.
Moore, T. E., J. W. Whitney, and W. K. Wallace, 1985, Cenozoic north-vergent tectonism in northeastern Alaska-indentor tectonics in Alaska?: Eos, Transactions, American Geophysical Union, v. 66, no. 46, p. 862.
Moore, T. E., A. Grantz, and S. M. Roeske, 1994a, Continent–ocean transition in Alaska: The tectonic assembly of eastern Denalia, *in* R. C. Speed, ed., Phanerozoic evolution of North American continent–ocean transitions: Geological Society of America, p. 399–441.
Moore, T. E., W. K. Wallace, K. J. Bird, S. M. Karl, C. G. Mull, and J. T. Dillon, 1994b, Geology of northern Alaska, *in* G. Plafker and H. C. Berg, eds., The geology of Alaska: Geological Society of America, The Geology of North America, v. G-1, p. 49–140.
Moore, T. E., W. K. Wallace, C. G. Mull, K. E. Adams, G. Plafker, and W. J. Nokleberg, 1997, Crustal implications of bedrock geology along the Trans-Alaska Crustal Transect (TACT) in the Brooks Range, northern Alaska: Journal of Geophysical Research, v. 102, no. B9, p. 20,645–20,684.
Mull, C. G., T. E. Moore, E. E. Harris, and I. L. Tailleur, 1994, Geologic map of the Killik River quadrangle, Brooks Range, Alaska: U.S. Geological Survey Open-File Report 94-679, scale 1:125,000, 1 sheet.
Mull, C. G., E. E. Harris, and P. Peapples, 2003a, Geologic map of the Cobblestone Creek–May Creek area, Brooks Range foothills, Alaska: Alaska Division of Geological and Geophysical Surveys Report of Investigations Map 2003-1, 1 sheet, scale 1:63,360, and booklet.
Mull, C. G., D. W. Houseknecht, and K. J. Bird, 2003b, Revised Cretaceous and Tertiary stratigraphic nomenclature in the central and western Colville basin, northern Alaska: U.S. Geological Survey Professional Paper 1673, http://pubs.usgs.gov/pp/p1673 (accessed April 15, 2006).
Mull, C. G., D. W. Houseknecht, G. H. Pessel, and C. P. Garrity, 2004, Geologic map of the Umiat quadrangle, Alaska: U.S. Geological Survey Scientific Investigations Map 2817-A, scale 1:250,000, 1 sheet.
North American Magnetic Anomaly Group, 2002, Magnetic anomaly map of North America: U.S. Geological Survey, scale 1:10,000,000, 1 sheet.
Nunn, J. A., M. Czerniak, and R. H. Pilger, Jr., 1987, Constraints on the structure of Brooks Range and Colville basin, northern Alaska, from flexure and gravity analysis: Tectonics, v. 6, no. 5, p. 603–617.
O'Sullivan, P. B., and W. K. Wallace, 2002, Out-of-sequence, basement-involved structures in the Sadlerochit Mountains region of the Arctic National Wildlife Refuge, Alaska— Evidence and implications from fission-track thermochronology: Geological Society of America Bulletin, v. 114, p. 1356–1378.
Payne, T. G., et al., 1952, Aeromagnetic map of Naval Petroleum Reserve No. 4 (Alaska), *in* Geology of the Arctic Slope of Alaska: U.S. Geological Survey Map OM-126, 3 sheets, scale 1:1,000,000.
Phillips, J., R. Saltus, and D. Daniels, 2002, Curvature depth analysis of gridded aeromagnetic data: European Geophysical Society XXVII General Assembly, Nice, April 21–26, 2002, http://www.cosis.net/abstracts/EGS02/02019/EGS02-A-02019-1.pdf (accessed June 29, 2006).
Phillips, J. D., 1997, Potential-field geophysical software for the PC-version 2.2: U.S. Geological Survey Open File Report 97-725, 34 p., http://pubs.usgs.gov/of/1997/ofr-97-0725/ (accessed April 15, 2006).
Phillips, J. D., 1999, An interpretation of proprietary aeromagnetic data over the northern Arctic National Wildlife Refuge and adjacent areas, northeastern Alaska, *in* The oil and gas resource potential of the Arctic National Wildlife Refuge 1002 Area, Alaska: U.S. Geological Survey Open File Report 98-34, chapter AM, 19 p.
Phillips, J. D., 2001, Designing matched bandpass and azimuthal filters for the separation of potential-field anomalies by source region and source type: Australian Society of Exploration Geophysicists, 15th Geophysical Conference and Exhibition Expanded Abstracts, CD-ROM, 4 p.
Phillips, J. D., R. W. Saltus, and R. L. Reynolds, 1999, Sources of magnetic anomalies over a sedimentary basin-preliminary results from the coastal plain of the Arctic National Wildlife Refuge, Alaska, *in* R. I. Gibson and P. S. Millegan, eds., Geologic applications of gravity and magnetics: Case histories: AAPG Studies in Geology 43, p. 130–134.
Potter, C. J., W. J. Perry, J. A. Grow, and M. W. Lee, 1999, Style and timing of thrust-faulting in the 1002 Area, Arctic National Wildlife Refuge— Chapter BD (Brookian deformation), *in* ANWR Assessment Team, The oil and gas resource potential of the 1002 Area, Arctic National Wildlife Refuge, Alaska: U.S. Geological Survey Open-File Report 98-34, CD-ROM, p. BD-1–BD-32.
Potter, C. J., J. A. Grow, W. J. Perry, Jr., T. E. Moore, P. B. O'Sullivan, J. D. Phillips, and R. W. Saltus, 2004, Tertiary thrust systems and fluid flow beneath the Beaufort coastal plain (1002 Area), Arctic National Wildlife Refuge, Alaska, U.S.A., *in* R. Swennen, F. Roure, and J. Granath, eds., Deformation, fluid flow and reservoir appraisal in foreland fold and thrust belts: AAPG Hedberg Series 1, p. 187–214.
Saltus, R. W., and K. J. Bird, 2003, Digital depth horizon compilations of the Alaskan North Slope and adjacent arctic regions:

U.S. Geological Survey Open-File Report 03-230, 21 p., http://pubs.usgs.gov/of/2003/ofr-03-230/ (accessed April 15, 2006).

Saltus, R. W., and G. C. Simmons, 1997, Composite and merged aeromagnetic data for Alaska— A Web site for distribution of gridded data and plot files: U.S. Geological Survey Open-File Report 97-520, 15 p., http://pubs.usgs.gov/of/1997/ofr-97-0520/ (accessed April 15, 2006).

Saltus, R. W., G. G. Connard, and P. L. Hill, 1999a, Alaska aeromagnetic compilation— Digital grids and survey data: U.S. Geological Survey Open-File Report 99-0502, 1 CD-ROM.

Saltus, R. W., T. L. Hudson, and G. G. Connard, 1999b, A new magnetic view of Alaska: Geological Society of America Today, v. 9, no. 3, p. 1–6.

Saltus, R. W., T. L. Hudson, and J. D. Phillips, 2001, Basement geophysical interpretation of the National Petroleum Reserve Alaska (NPRA), northern Alaska: U.S. Geological Survey Open-File Report 01-0476, 3 poster panels with supplementary text, http://pubs.usgs.gov/of/2001/ofr-01-0476/ (accessed April 15, 2006).

Saltus, R. W., T. L. Hudson, J. D. Phillips, C. Kulander, J. Dumoulin, and C. Potter, 2002, Basement geology of the National Petroleum Reserve Alaska (NPRA), northern Alaska: U.S. Geological Survey Open-File Report 02-0127, 11 p., http://pubs.usgs.gov/of/2002/ofr-02-0127/ (accessed April 15, 2006).

Sherwood, K. W., P. P. Johnson, J. D. Craig, S. A. Zerwick, R. T. Lothamer, D. K. Thurston, and S. B. Hurlbert, 2002, Structure and stratigraphy of the Hanna Trough, U.S. Chukchi Shelf, Alaska, *in* E. L. Miller, A. Grantz, and S. L. Klemperor, eds., Tectonic evolution of the Bering Shelf–Chukchi Sea–Arctic Margin and adjacent landmasses: Geological Society of America Special Paper 360, p. 39–66.

Simpson, R. W., R. C. Jachens, R. J. Blakely, and R. W. Saltus, 1986, A new isostatic residual gravity map of the conterminous United States with a discussion on the significance of isostatic residual anomalies: Journal of Geophysical Research, v. 91, no. B8, p. 8348–8372.

Sims, P. K., R. W. Saltus, and E. D. Anderson, 2005, Preliminary Precambrian basement structural map of the continental United States— An interpretation of geologic and aeromagnetic data: U.S. Geological Survey Open-File Report 2005-1029, http://pubs.usgs.gov/of/2005/1029/ (accessed April 15, 2006).

Sleep, N. H., and K. Fujita, 1997, Principles of geophysics: Malden, Massachusetts, Blackwell Science, 586 p.

Spurlin, J. H., 1993, Regional isostasy: Ph.D. thesis T-4366, Colorado School of Mines, Golden, Colorado, 186 p.

Syberg, F. J. R., 1972, A Fourier method for the regional-residual problem of potential fields: Geophysical Prospecting, v. 20, p. 47–75.

Verma, M. K., K. J. Bird, P. H. Nelson, and R. C. Burruss, 2005, Evaluation of the stranded Kavik gas field, north slope of Alaska: U.S. Geological Survey Open-File Report 2005-1389, one plate, http://pubs.usgs.gov/of/2005/1389/ (accessed April 15, 2006).

Watts, A. B., 2001, Isostasy and flexure of the lithosphere: Cambridge, United Kingdom, Cambridge University Press, 458 p.